JPRS L/8569
13 July 1979
(FOUO 1/79)

USSR Report

PHYSICS AND MATHEMATICS

QUANTUM ELECTRONICS

FBIS FOREIGN BROADCAST INFORMATION SERVICE

APPROVED FOR RELEASE: 2007/02/09: CIA-RDP82-00850R000100070014-8

NOTE

JPRS publications contain information primarily from foreign newspapers, periodicals and books, but also from news agency transmissions and broadcasts. Materials from foreign-language sources are translated; those from English-language sources are transcribed or reprinted, with the original phrasing and other characteristics retained.

Headlines, editorial reports, and material enclosed in brackets [] are supplied by JPRS. Processing indicators such as [Text] or [Excerpt] in the first line of each item, or following the last line of a brief, indicate how the original information was processed. Where no processing indicator is given, the information was summarized or extracted.

Unfamiliar names rendered phonetically or transliterated are enclosed in parentheses. Words or names preceded by a question mark and enclosed in parentheses were not clear in the original but have been supplied as appropriate in context. Other unattributed parenthetical notes within the body of an item originate with the source. Times within items are as given by source.

The contents of this publication in no way represent the policies, views or attitudes of the U.S. Government.

For further information on report content call (703) 351-2938 (economic); 3468 (political, sociological, military); 2726 (life sciences); 2725 (physical sciences).

APPROVED FOR RELEASE: 2007/02/09: CIA-RDP82-00850R000100070014-8

JPRS L/8569

13 July 1979

USSR REPORT

PHYSICS AND MATHEMATICS

(FOUO 1/79)

QUANTUM ELECTRONICS

Moscow KVANTOVAYA ELEKTRONIKA in Russian Vol 6 No. 4(82), Apr 79
pp 747-758, 765-781, 851-852, 864-867

CONTENTS PAGE

PHYSICS

PHYSICS

UDC 621.378.325

INFLUENCE THAT MIXING EFFECTS HAVE ON THE ENERGY CHARACTERISTICS OF A SELF-CONTAINED CW CHEMICAL HF LASER

Moscow KVANTOVAYA ELEKTRONIKA in Russian Vol 6, No 4(82), Apr 79 pp 747-758

[Article by A. A. Stepanov and V. A. Shcheglov, Physics Institute imeni P. N. Lebedev, Academy of Sciences USSR, Moscow]

[Text] A self-contained chemical HF laser of diffusion type is calculated on the basis of boundary layer equations. The authors discuss the particulars of the method of calculation. An investigation is made of the way that the energy characteristics of the laser depend on the parameters of the system. Major emphasis is placed on the influence of factors that control the process of mixing of the oxidizer and fuel jets. The results of the work can be used in practical optimization of the energy characteristics of a cw chemical HF laser.

1. Introduction

With the development of supersonic chemical HF lasers that occupy a leading place in the field of circulating laser systems with chemical excitation, there has been an expansion of the class of theoretical problems that are in urgent need of solution and have direct practical significance. The energy parameters of lasers of this class depend appreciably on both kinetic and gasdynamic processes that have an influence on the formation of the active medium as chemically active jets are mixed. However, while the area of the chemical and vibrational kinetics of HF lasers has been fairly well covered, the same cannot be said of the gasdynamic phenomena that are typical of such a system, which is due in large part to the complexity of adequate calculation of the gasdynamic flow pattern.

One of the following approaches is generally used in theoretical investigation of cw chemical lasers: one-dimensional (instantaneous mixing model [Ref. 1,]); quasi one-dimensional (of the flame-front model type [Ref. 8-12, 18-20]); an approach in which the mixing process is described by boundary layer equations [Ref. 2, 3, 5-7, 14-16]. In a more general approach, the

calculation of the diffusion HF laser should be based on Navier-Stokes equations (the corresponding equations for the plane and cylindrical cases are presented in Ref. 17). However, such an approach imposes excessive demands on the computer and therefore at present can scarcely be recommended for studying energy characteristics*.

In contrast to the one-dimensional approach, quasi one-dimensional models account for the finiteness of the rate of mixing of reagents; however, the description of processes in the laser zone remains one-dimensional. Let us note that these models have been used to get a number of practically important results both directly in analytical form [Ref. 8-10, 12], and with the use of comparatively simple numerical calculations [Ref. 18-20]. At the same time, mention should be made of the openness of quasi one-dimensional models, in virtue of which the diffusion mixing length $x_д$ (see for instance Ref. 8, 12) must be determined from supplementary conditions. This circumstance is obviously eliminated when the self-consistent problem is solved on the basis of boundary layer equations. This approach with predetermined boundary conditions gives more complete information on the distribution of gasdynamic parameters with respect to current in the resonator cavity and on the influence that external factors have on the energy characteristics of the laser.

In this article a self-contained chemical HF laser of diffusion type is calculated on the basis of boundary layer equations. Major emphasis in the analysis is placed on the influence of factors that control the process of mixing of the gas streams: the space period of the nozzle cascade, the ratio between the transverse dimensions of the jets of oxidizer and fuel, the overall pressure in the flow, and the initial temperatures of the jets. The literature is essentially devoid of such information, but at the same time this data is the basis for choosing the specific parameters of a laser system when optimizing its energy characteristics. The results apply to an HF laser in which excitation is achieved by a single-stage chemical process $F+H_2 \rightarrow HF+H$ (the "cold" reaction mechanism).

2. Fundamental Kinetic Processes

A peculiarity of a self-contained supersonic chemical HF laser is the generation of active centers (fluorine atoms) in the power section due to the heat released as the corresponding fuel burns in an atmosphere of excess fluorine-containing reagent. Usually this goal is met by the combustion reaction $\alpha F_2 + D_2 \rightarrow 2DF + (\alpha - 1)F_2$.

In calculating the output parameters of the laser, we took consideration of the following kinetic processes in the laser zone: 1) the pumping reaction $F+H_2 \rightarrow HF(v)+H$, where $v = 1-3$ is the number of the vibrational level of HF;

*Let us mention Ref. 13, where the first attempts have been made at using Navier-Stokes equations in application to the HF laser. Although these papers do not contain calculations of energy parameters, they are of procedural interest.

2) recombination of F and H atoms; 3) HF-HF and HF-H_2 vibrational exchange; 4) collisional deactivation of HF and H_2 molecules; 5) radiative transitions of HF(v) molecules (the P-branches of the vibrational bands $v \to v-1$, $v = 1-3$ are considered).

Let us make a few comments relative to vibrational kinetics. Since a considerable admixture of deuterium fluoride molecules is present in the primary (oxidative) flow, it is also necessary to consider the nonresonant HF-DF vibrational exchange. This process is directional in nature with transfer of vibrational energy from HF to DF (the vibrational quantum of the HF molecule is appreciably higher); therefore under the given conditions the reverse flow of energy (from DF to HF) is low and can be ignored. This circumstance enables us to combine the given process with the process of collisional relaxation of HF on DF molecules, and to use as the constants of such a process the overall constant of VV' exchange and VT relaxation of HF molecules on DF. Let us note that in the case of nonresonant HF-H_2 vibrational exchange an analogous simplification is no longer justified since the direction taken by this process is essentially the reverse, and the concentration of H_2 molecules in the total mixture is rather high under typical conditions.

For the sake of simplicity, a harmonic approximation was used in describing vibrational kinetics; the rate constants of the corresponding reactions are given in Ref. 20. For the overall constant of relaxation of HF on DF, just as in Ref. 18, 19, we took the expression $k_{VT}(DF) = 1.3 \cdot 10^{17}/T^{1.9}$ cm^3/(mole·s). Let us note that even though the HF level with $v = 4$ is not populated during pumping, nevertheless it is difficult to account correctly for VV exchange in HF without considering this level. This situation compels us to account for no less than five vibrational levels of HF ($v = 0-4$) in calculations of a laser on the "cold" reaction.

The energy characteristics of the HF laser with optical cavity were calculated as usual on the basis of a quasi-steady state method. It was assumed that in each fixed cross section along the flow, lasing in any of the investigated bands $v \to v-1$ takes place only on a single vibrational-rotational transition of the P-branch v, $j_v - 1 \to v-1$, j_v. The rotational quantum number j_v that corresponds to this transition was selected from the condition of the maximum gain in the given band as averaged over the period of the nozzle structure.

3. Equations of Gas Dynamics

The supersonic cw chemical HF laser facility (Fig. 1) includes a large number of small plane-parallel nozzles with alternating jets of oxidizer (F) and fuel (H_2), and therefore it can be assumed that the properties of the active medium in the flat cavity vary periodically along the Z axis. This permits us to calculate the stimulated emission for a single half-period h_* (shaded region on Fig. 1), and to take account of the total length L_a of the active medium in the threshold condition.

The general equations of a two-dimensional boundary layer are well known [Ref. 21-23, and take the form

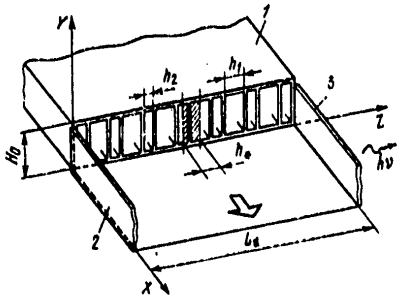

Fig. 1. Simplified diagram of the HF diffusion laser: 1--nozzle module; 2, 3--mirrors of the cavity

$$\text{a)}\quad \frac{\partial}{\partial x}(\rho u)+\frac{\partial}{\partial z}(\rho v)=0\ ;$$

$$\text{b)}\quad \rho u\frac{\partial u}{\partial x}+\rho v\frac{\partial u}{\partial z}=-\frac{dp}{dx}+\frac{\partial}{\partial z}\left(\mu\frac{\partial u}{\partial z}\right);$$

$$\text{c)}\quad \rho u\frac{\partial h}{\partial x}+\rho v\frac{\partial h}{\partial z}=u\frac{dp}{dx}+\mu\left(\frac{\partial u}{\partial z}\right)^2+\frac{\partial}{\partial z}\left(\lambda\frac{\partial T}{\partial z}\right)+$$
$$+\frac{\partial}{\partial z}\left(\rho\sum_i h_i D_i\frac{\partial C_i}{\partial z}\right)-\sum_v g^l_{v,v-1}I_{v,v-1};$$

$$\text{d)}\quad p=\rho RT/W;$$

$$\text{e)}\quad \rho u\frac{\partial C_i}{\partial x}+\rho v\frac{\partial C_i}{\partial z}=\dot{w}_i+\frac{\partial}{\partial z}\left(\rho D_i\frac{\partial C_i}{\partial z}\right),$$

where u and v are the components of flow velocity along the X and Z axes respectively; ρ is the mass density of the mixture; p is pressure; h is specific enthalpy; T is temperature; μ, λ and D_i are transfer coefficients; $C_i=\rho_i/\rho$ is the relative mass concentration of the i-th component; the $\dot{w}_i$ describe the processes of chemical, vibrational and radiative kinetics and have a standard form (see for instance Ref. 17); W is the molecular weight of the mixture.

It is assumed in the given equations that diffusion of the jets is laminar. It should be noted that when discharge conditions are close to the calculated values, the flow region beyond the nozzle tips as a rule breaks down into three subregions. In the immediate vicinity of the nozzle is a region of laminar flow, which is followed by a transition section, and finally a region of developed turbulence. Experiments show that at typical working pressures of about 3-10 mm Hg and discharge velocities of 2-4 km/s there is not enough time for the turbulent mode to develop in the laser zone (characteristic width $\Delta x_{\text{л}}\sim$ 3-10 cm), and therefore accounting for turbulent effects in the investigated cases should not appreciably change the results of the calculations.

As a result of heat liberated in the flow, directed motion of the gas along the X axis is accompanied by a tendency toward expansion in the transverse directions Y and Z (see Fig. 1). Since the width L_a along the Z axis is rather large (of the order of 20-40 cm or more), the effects of expansion in this direction can be ignored. At the same time, the height H_0 of the flow in different nozzles fluctuates over wide limits, and under certain conditions the degree of expansion of the gas in the direction of the Y axis may be appreciable. Thus the gas flow in the cavity region, generally speaking, should be treated as three-dimensional. However, in two limiting cases that are investigated in practice, we can restrict ourselves to a two-dimensional approach.

For instance if $H_0 \gg 2\Delta x_{\text{п}}/M$, where M is the Mach number at the nozzle tip, the transit time of the cavity is not sufficient for thermal perturbations to propagate from the inner layers of the flow to the peripheral regions, and gas expansion in the direction of the Y axis can be disregarded. In this case the cross sectional area of the flow does not change ($S(x) = \text{const}$), and the gas pressure along the X axis increases in proportion to the average temperature of the mixture over the cross section: $p \sim h^{-1}\int_0^h T dz$. The other limiting case ($H_0 \ll 2\Delta x_{\text{п}}/M$) corresponds physically to free expansion of the gas in the direction of the Y axis under the action of internal heat liberation. In this case, the pressure of the mixture along the flow does not change ($p(x) = \text{const}$), and the density of the mixture ρ decreases. For an HF laser based on the "cold" reaction with typical helium dilutions of the mixture (from five- to fifteen-fold) these two flow regimes differ comparatively weakly in the energy sense because thermal effects in this instance are still not too appreciable. For the sake of definiteness it was assumed in the calculations that $p(x) = \text{const}$.

In the given situation, the usual equation of continuity for the mixture as a whole [relation a)] cannot be used in the customary form since it does not account for free expansion of the gas in the direction of the Y axis. It can be shown that the true equation of continuity that satisfies the law of mass conservation in integral form, in the "quasi two-dimensional" approximation takes the form

$$\frac{\partial}{\partial x}(\rho u l_y(x)) + l_y(x)\frac{\partial}{\partial z}(\rho v) = 0. \qquad (1)$$

The quantity $l_y(x) = H(x)/H_0$ that characterizes the degree of expansion of the gas along the Y axis is determined, generally speaking, by using the integral law of mass conservation.

When integrating the boundary layer equations it is advisable as always to convert from cartesian coordinates x, z to the variables ξ, ψ by using the relations

$$\xi = x, \quad \psi = l_y(x)\int_0^z \rho u dz. \qquad (2)$$

The boundary layer equations take a simpler form in the new variables.

1. The equation of continuity for individual components

$$\frac{\partial C_i}{\partial \xi} = l_\nu^2(\xi)\frac{\partial}{\partial \psi}\left(\rho^2 u D_i \frac{\partial C_i}{\partial \psi}\right) + \dot{w}_i/\rho u, \tag{3}$$

where i = F, H_2, He, H, DF, HF(v) (v = 0-4).

2. The equations of motion

$$\frac{\partial u}{\partial \xi} = l_\nu^2(\xi)\frac{\partial}{\partial \psi}\left(\rho u \mu \frac{\partial u}{\partial \psi}\right). \tag{4}$$

3. The equation of energy conservation

$$c_p \frac{\partial T}{\partial \xi} = l_\nu^2(\xi)\left\{\frac{\partial}{\partial \psi}\left(\rho u \lambda \frac{\partial T}{\partial \psi}\right) + \rho u \frac{\partial T}{\partial \psi}\left(\sum_i c_{p_i}\rho D_i \frac{\partial C_i}{\partial \psi}\right)\right\} + \dot{w}_T, \tag{5}$$

where c_p, c_{p_i} are the respective specific heats of the mixture and the i-th component at constant pressure.

4. The equation of state

$$p = \rho RT/W = \text{const.} \tag{6}$$

In a case like this, the complete equation of continuity (1) is satisfied automatically, and equations (1), (2) and condition $v(x,0) = v(x,h_*) \equiv 0$ imply

$$\psi_* = \int_0^{h_*} \rho u l_\nu(x)\,dz = \text{const.}$$

In the case of the equations of continuity for individual vibrational levels of HF molecules, we have for $\dot{w}_{HF}(v)$ (v = 0-4)

$$\dot{w}_{HF}(v) = \dot{w}_{хим}(v) + \dot{w}_{рад}(v),$$

[note: subscript хим = chemical, рад = radiative]

where

$$\dot{w}_{рад}(v) = (W_{HF}/N_a h\nu_{HF})\left[g^{J_{v+1}}_{v+1,v} I_{v+1,v} - g^{J_v}_{v,v-1} I_{v,v-1}\right],$$
$$\dot{w}_{хим}(v) = \rho^2 W_{HF}\left[Q_{хим}(v) + Q_{VT}(v) + Q^{(1)}_{VV}(v) + Q^{(2)}_{VV}(v)\right].$$

Here W_i is the molecular weight of the i-th component, $g^j_{v,v-1}$ is the local gain of the active medium on vibrational-rotational transition v,j-1→v-1,j; $I_{v,v-1}$ is emission intensity on the same transition; $Q_{хим}(v)$ describes chemical processes, and in particular pumping of the corresponding level, $Q_{VT}(v)$ -- vibrational-translational relaxation of HF, and $Q^{(1)}_{VV}(v)$ and $Q^{(2)}_{VV}(v)$ -- vibrational-vibrational exchanges of HF-HF and HF-H_2 respectively.

In order to close the system of equations of continuity for $C_{HF}(v)$ it is necessary to assign the algorithm for calculating the emission intensities $I_{v,v-1}$ of individual bands, and also to introduce an equation for the vibrational energy contained in the H_2 molecules (i. e. for the number of vibrational quanta of H_2 per gram of the mixture):

$$\frac{\partial \varkappa_{H_2}}{\partial \xi} = l_y^2(\xi)\frac{\partial}{\partial \psi}\left(\rho^2 u D_l \frac{\partial \varkappa_{H_2}}{\partial \psi}\right) + \dot{\omega}_{\varkappa_{H_2}}/\rho u, \qquad (7)$$

where $\dot{\varkappa}_{H_2} = \sum_v v\dot{C}_{H_2}(v)/W_{H_2}$, and the term $\dot{\omega}_{\varkappa_{H_2}}$ accounts for VV' exchange of HF-H_2, and VT relaxation of H_2 molecules.

Moreover, the quantity $\dot{w}_T$ that appears in energy conservation equation (5) can be represented in the following form (let us note that the radiation term in $\dot{w}_T$ can be eliminated as a result of simple transformations using the equations of continuity for the individual components without regard to the deficiency of HF rotational quanta [Ref. 20]):

$$\dot{\omega}_T = \rho u \mu l_y^2(\xi)\left(\frac{\partial u}{\partial \psi}\right)^2 - (\rho u)^{-1}\left\{\sum_i h_i \dot{\omega}_i + N_a h\nu_{H_2}\dot{\omega}_{\varkappa_{H_2}} + (N_a h\nu_{HF}/W_{HF})\sum_v v\dot{\omega}_{\text{хим}}(v)\right\},$$

where $h_i = h_i^0 + c_{p_i}T$ is specific enthalpy, h_i^0, $h\nu_i$ are the specific heat of formation and the energy of a vibrational quantum of the i-th component, N_a is Avagadro's number.

To determine the degree of expansion of the flow in the direction of the Y axis, let us refer to the expression for ψ_*. Considering that $l_y(x=0) = 1$, we get

$$l_y(\xi) = \int_0^{h_*} \rho_0 u_0 dz \Big/ \int_0^{h_*} \rho u dz = \psi_*^{-1}\int_0^{\psi_*} (\rho_0 u_c/\rho u)d\psi, \qquad (8)$$

where ρ_0 and u_0 are the initial distributions of density and velocity of the mixture at the outlet of the nozzle module.

The transfer coefficients that figure in equations (3)-(8) -- the coefficient of dynamic viscosity of a multicomponent mixture μ and the effective coefficients of diffusion of individual components D_i -- were determined from Wilkey's formulas [Ref. 21, 24] that relate the effective transfer coefficients D_{ij} and μ_i for binary mixtures to those for the multicomponent mixture (see also Ref. 13, 17). The temperature dependences of D_{ij} and μ_i are taken directly from Ref. 17. The coefficient of thermal conductivity λ was calculated in terms of μ on the basis of gas-kinetic theory.

The boundary conditions for the investigated system of equations are based on accounting for the periodicity of the flow structure. At $\psi = 0$ and ψ_* we have

$$\frac{\partial u}{\partial \psi} = \frac{\partial T}{\partial \psi} = \frac{\partial \rho}{\partial \psi} = \frac{\partial C_i}{\partial \psi} = 0.$$

The conditions at the outlet of the nozzle module, i. e. where $\xi = 0$, take the form $u = u_0(\psi)$; $T = T_0(\psi)$; $\rho = \rho_0(\psi)$; $C_i = C_i^0(\psi)$.

Now let us briefly take up the question of calculating the intensities of the individual bands $I_{v,v-1}$ in the optical cavity in the boundary layer

equation approximation [Ref. 5, 17]. As usual, we denote the threshold gain in the cavity by $g_{п} = l_{п}^{-1} \ln (r_0 r_1)^{-1/2}$, where r_0 and r_1 are the reflectivities of the mirrors. Knowing the local gain of the active medium (here we use the generally accepted spectroscopic notation)

$$g^{l}_{v,v-1}(\xi, \psi) = \Phi_{vj}(\xi, \psi)\,[C_{HF}(v) - \beta_j C_{HF}(v-1)], \qquad (9)$$

where

$$\Phi_{vj} = \frac{\rho N_0}{W_{HF}} \frac{c^2 A^{l}_{v,v-1}}{8\pi\nu^2 \Delta\nu_D} (\ln 2/\pi)^{1/2} \frac{\theta_{rot}}{T}(2j-1)\exp\left[-\frac{\theta_{rot}}{T} j(j-1)\right],$$

$$\beta_j = \exp\left(-\frac{2\theta_{rot}}{T} j\right),$$

we introduce the average gain with respect to the period of the structure $G^{l}_{v,v-1}$, setting

$$G^{l}_{v,v-1}(\xi) \approx \psi_*^{-1} \int_0^{\psi_*} g^{l}_{v,v-1}\, d\psi.$$

Assuming that in the mode of steady-state lasing

$$G^{l}_{v,v-1}(\xi) \approx g_{п},$$

we differentiate this expression with respect to ξ with consideration of (9) and (3) to get a system of algebraic equations for determining emission intensities $I_{v,v-1}$. To simplify the calculations it is advisable to use the fact that the quantities Φ_{vj}, β_j and ρ_u as compared with $\dot{w}_{хим}(v)$ and $\dot{w}_{рад}(v)$ are weakly dependent on the coordinates. Then with consideration of the boundary conditions for $C_{HF}(v)$ we can represent the system of algebraic equations for $I_{v,v-1}$ as follows (see also Ref. 17):

$$I_{v+1,v} - (1 + \beta^{*}_{j_v}) I_{v,v-1} + \beta^{*}_{j_v} I_{v-1,v-2} = -F_v, \qquad (10)$$

where

$$F_v(\xi) = (N_0 h\nu_{HF} / g_{п} W_{HF} \psi_*) \int_0^{\psi_*} [\dot{w}_{хим}(v) - \beta_{j_v} \dot{w}_{хим}(v-1)]\, d\psi;$$

$$\beta^{*}_j = \exp\left(-\frac{2\theta_{rot}}{T_*} j\right); \quad T_* \approx \psi_*^{-1} \int_0^{\psi_*} T\, d\psi.$$

After determining the emission intensities of individual bands, calculation of the energy characteristics of the HF laser presents no difficulties [Ref. 12], and we will not discuss it.

System of equations (3)-(10) was solved by using a difference approximation in a Crank-Nicholson scheme [Ref. 25-27]. A sweep method was used in addition to the simple iteration procedure proposed in Ref. 25, 26 to resolve the system of quasilinear algebraic equations for net-point functions. Simpson's method was used to calculate the integrals in relations (8), (10). Calculations by the described method were done on the BESM-6 computer. The integration step with respect to the transverse coordinate was taken as fixed (as a rule, 20 points were taken along ψ), and the step with respect to the X axis was varied depending on the rate of kinetic processes. The typical time for calculating one variant did not exceed 30-40 minutes.

4. Results of the Calculations

Since the oxidizer stream at the nozzle module outlet contains particles of F_2, DF and He in addition to fluorine atoms, we introduce the following parameters for unambiguous characterization of the composition of the flow of oxidizer:

$$\alpha_F = \xi_F/(\xi_F + 2\xi_{F_2}); \quad \beta_{He} = 2\xi_{He}/(\xi_F + 2\xi_{F_2}), \quad \beta_{DF} = 2\xi_{DF}/(\xi_F + 2\xi_{F_2}),$$

where $\xi_i = N_i/N = W_1C_i/W_i$ are the relative concentrations of particles in the oxidizer flow. Henceforth we will consider only the case of the "cold" reaction laser, and will assume $\alpha_F = 1$.

The case with respect to which the parameters of the system were varied is characterized by the following data:

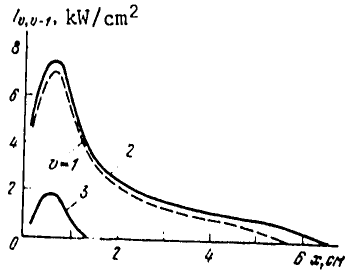

Fig. 2. Distribution of the emission intensities of individual bands along the lasing zone in a flat cavity.

a) pressure at the nozzle tip p = 5 mm Hg, length of the active medium L_a = 20 cm, half-width of the nozzle period $h_* = 0.25$ cm, ratio of the widths of the individual jets $h_1/h_2 = 2$, reflectivities of the mirrors $r_0 = 0.98$ and $r_L = 0.75$;

b) for the primary flow $T_1 = 275$ K, $u_1 = 2.7$ km/s, $\beta_{He} = 10$ and $\beta_{DF} = 2$;

c) for the secondary flow $T_2 = 120$ K, $u_2 = 2.3$ km/s.

The distribution of emission intensities $I_{v,v-1}$ within the active medium in the lasing mode for the given case is shown in Fig. 2. Let us note also that calculations imply that the most intense lines in the emission spectrum correspond to transitions $P_v(5)$ and $P_v(6)$ for v = 1, 2.

Variation of the width of a period of the nozzle structure. With an increase in h_* (i. e. with a reduction in the total number of jets at fixed L_a), the

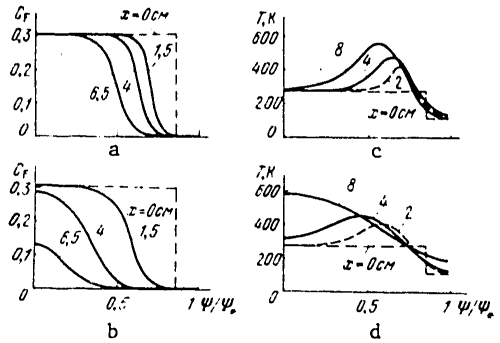

Fig. 3. Transverse distributions of mass concentration of atomic fluorine C_F (a, b) and temperature of the mixture T (c, d) in different cross sections along the flow at $h_* = 0.5$ cm (a, c) and 0.25 cm (b, d).

intermixing of reagents slows down and less and less atomic fluorine (and he ce chemical power stored in the flow) has time to be used in the laser zone. This is graphically confirmed by the results shown in Fig. 3. When $h_* = 0.25$ cm (Fig. 3b, d), up to 80% of the fluorine available in the flow is burned up in the lasing zone; when h_* is doubled (Fig. 3a, c) the degree of utilization of oxidizer drops to 30-35%. In such a situation, the output energy characteristics of the HF laser (chemical efficiency $\eta_{хим}$, specific laser energy E_0 and so forth) deteriorate noticeably with increasing h_* (Fig. 4a).

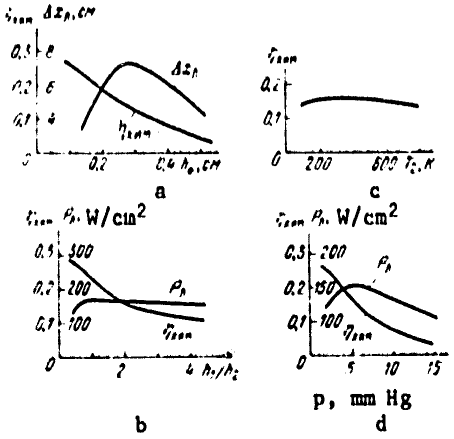

Fig. 4. Dependence of the energy characteristics of the HF laser on the period of the structure h_* (a), the ratio of the widths of the jets h_1/h_2 (b), the fuel temperature T_2 (c) and the pressure p in the cavity (d).

It should be noted that according to the given results the chemical efficiency varies over a fairly wide range in approximate inverse proportion to the width of the period of the structure, i. e. $\eta_{хим} \sim h_*^{-1}$. Attention should also be called to the fact that the width of the lasing zone has a typical dependence on h_*. Fig. 4a shows that this dependence has an extremum. This can be attributed to the fact that as $h_* \to 0$ (i. e. at the limit of instantaneous mixing) the width of the laser zone is determined by the characteristic length of the chemical reaction [Ref. 8, 12], which is usually short. On the other hand under conditions of slow mixing (h_* large) the chemical pumping rate is low and the temperature of the mixture rises very slowly, and therefore relaxation processes become more significant and the width of the lasing zone again begins to decrease. Clearly the specific position of the maximum on the curve for $\Delta x_{\text{л}}(h_*)$ depends both on the pressure and on the composition of the mixture as well as on its initial temperature.

Variation of the width of the jets. Variations of the ratio h_1/h_2 while the period $h_* = (h_1 + h_2)/2$ remains fixed at 0.25 cm are shown in Fig. 4b. We note that the basic conclusions in this case as well differ but little

from those of the preceding case. For instance as h_1 increases, the mass flow of atomic fluorine and the reserve of chemical power (per sq. cm of cross sectional area of the nozzle), of course, increase; but in this case a smaller and smaller part of the fluorine available in the mixture has time to react in the laser zone since the hydrogen in this case does not have time to penetrate into the oxidizer (diffusion of fluorine into the hydrogen stream is less significant). At low h_1 the atomic fluorine is nearly totally expended and the chemical efficiency of the laser increases noticeably; notwithstanding, the total power of stimulated emission still falls since the stored power P_{XHM} falls off. At large h_1/h_2, the lasing power remains practically unchanged over a fairly wide range of h_1/h_2.

Variation of initial fuel temperature. As the molecular hydrogen is heated in the gas generator chamber the temperature at the nozzle tip can be varied over a wide range. It would seem that for diffuse mixing one should expect an improvement in the energy characteristics of a chemical laser with an increase in T_2. However, calculations show that in reality no such effect is observed (Fig. 4c). This can apparently be attributed to the fact that mixing of the reagents takes place chiefly as a consequence of diffusion of H_2 into the oxidizer flow, and the rate of this process is determined primarily by the temperature of the oxidizer stream and the thermal effect of the reaction. It should be noted that analogous results have been found in experimental investigation of the rate of mixing of fluorine with cold and hot H_2 [Ref. 28].

Pressure variation in the resonator cavity. An investigation of the way that the energy parameters of a diffusion laser depend on pressure within the framework of the quasi one-dimensional model gives the following results The chemical efficiency of an HF laser decreases with increasing p ($n_{XHM} \sim 1/p$), while the power of stimulated emission at low pressures first rises, and then reaches saturation and ceases to change [Ref. 8, 10, 12, 20]. A more exact analysis based on boundary layer equations shows that the actual dependence of energy characteristics on pressure should nevertheless be somewhat different (Fig. 4d). For instance chemical efficiency with rising pressure decreases (under typical conditions) somewhat more rapidly than in the quasi one-dimensional model, while the lasing power, after reaching an extremum, then begins, generally speaking, to fall off. We can readily see that these results are intimately related to the influence that thermal effects have on the process of mixing of reagents. With deterioration of mixing conditions (with increasing p), there is naturally a reduction in the rate of heat release in the flow, and other things being equal the rise in temperature of the mixture slows down. Since the diffusion coefficients D_i depend noticeably on temperature, this circumstance is what leads to the observed effect. (Let us note that a temperature rise also leads to a reduction in the rate of relaxation of HF molecules on HF and DF.)

This analysis implies that with an increase in the initial temperature of the mixture (primarily T_1) the pressure dependence of the output power should be weaker. Finally, in the case of considerable dilution of the mixture with

helium (when the part played by thermal effects is practically insignificant) the relation $P_{\Pi}(p)$ should have approximately the same form as in the quasi one-dimensional model.

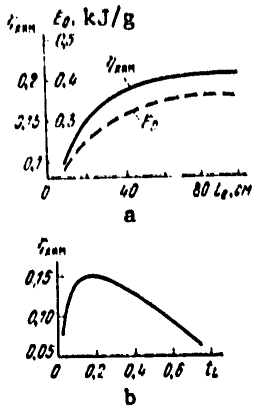

Fig. 5. Dependence of the energy characteristics of the laser on total width of the nozzle module L_a (a) and the transmissivity t_L of the output mirror (b)

Variation of the length of the active medium. Usually selection of the total width L_a of the nozzle module is dictated chiefly by the power that is to be provided by the facility being designed. Under these conditions it is important that with increasing L_a up to about 0.6 m a noticeable improvement can be seen in the specific energy characteristics of the HF laser (Fig. 5a). The increase of efficiency in this case is due to the reduction of the lasing threshold in the cavity and to the increase of emission density in the active medium. The latter leads to a more significant role played by collisional deactivation of HF molecules with conversion of a greater part of the vibrational energy to radiation. It should be noted that the emission density in the active medium increases practically in proportion to L_a, and therefore the loads on the mirrors become very heavy at large L_a.

Let us also say a few words about the influence of a number of other parameters on the energy characteristics of the cw HF laser.

The dependence of efficiency on the transmissivity of the output mirror t_L has the usual form (Fig. 5b, absorption in the mirrors was taken as $a_0 = a_L = 0.02$ in the calculations). Nevertheless, consideration should be given to the fact that over a fairly wide range of t_L from about 0.1 to 0.3 the chemical efficiency varies weakly. This circumstance can be utilized to reduce radiant loads on the mirrors, since the radiation density in the cavity drops sharply with increasing t_L.

As a rule, an increase in the temperature of the oxidizer flow T_1 over a range of about 200-400 K has a favorable influence on the output parameters of the HF laser, leading to increased efficiency. Nonetheless, of greater importance is the fact that with increasing T_1 the output characteristics become less critical to pressure in the cavity, enabling operation in the high-pressure region. As has already been noted, the main reason for such an improvement in the HF laser characteristics is associated on the one hand with an increase in mixing rate, and on the other hand with a reduction in the rate of collisional deactivation of HF. Besides, at high temperatures of the mixture, lasing takes place on vibrational-translational transitions that correspond to higher values of the rotational quantum number. And it is known that this may also be conducive to increased efficiency [Ref. 18].

In conclusion let us note the following. In our research major emphasis has been placed on the most fundamental problems relating to optimization of the operation of a diffusion laser. In this connection, effects relating to the presence of boundary layers on the nozzle walls have been totally left out of consideration. Of course such effects lead to a reduction in the energy characteristics of the system, and this must be taken into consideration. Since adequate calculation of the system in its entirety, including the nozzle module, is very cumbersome, in a real situation it is advisable to carry out such a calculation in two stages. This gives a more or less complete picture of the gasdynamic parameters at the outlet from the nozzle module, that can be easily taken into consideration in subsequent calculation of the energy characteristics of a cw HF laser.

REFERENCES

1. G. Emanual, JQSRT, Vol 11, 1971, p 1481.

2. R. Hofland, H. Mirels, AIAA J., Vol 10, 1972, p 420, 1271.

3. W. S. King, H. Mirels, AIAA J., Vol 10, 1972, p 1647; AIAA Paper No 72-146 1972.

4. G. E. Emanual, N. Cohen, T. A. Jacobs, JQSRT, Vol 13, 1973, p 1365.

5. A. W. Ratliff, J. Thoenes, AIAA Paper, No 73-644, 1973; No 74-225, 1974.

6. R. Tripodi, L. J. Coulter, B. R. Bronfin, L. S. Cohen, AIAA J, Vol 13, 1975, p 776; AIAA Paper No 74-224, 1974.

7. R. R. Mikatarian, A. J. McDanal, AIAA Paper No 75-39. 1975.

8. H. Mirels, R. Hofland, W. S. King, AIAA J., Vol 11, 1973, p 156.

9. H. Mirels, AIAA J., Vol 13, 1975, p 785; Vol 14, 1976, p 930.

10. J. E. Broadwell, APPL. OPTICS, Vol 13, 1974, p 962.

11. R. J. Hall, IEEE J., QE-12, 1976, p 453.

12. A. A. Stepanov, V. A. Shcheglov, ZHURNAL TEKHNICHESKOY FIZIKI, Vol 46, 1976, p 563; Preprint, Lebedev Physics Institute, Moscow, 1975, No 134.

13. A. P. Kothary, J. D. Andersen, AIAA J., Vol 14, 1976, p 707; Vol 15, 1977, p 92.

14. V. I. Golovichev, N. G. Preobrazhenskiy, V. A. Yasakov, ARCHIV. MECHANICS, Vol 28, 1976, p 733.

15. V. I. Golovichev, N. G. Preobrazhenskiy, FIZIKA GORENIYA I VZRYVA, Vol 13, 1977, p 366; in "Gazovyye lazery," Novosibirsk, Nauka, 1977, pp 83-104.

16. V. K. Bayev, V. I. Golovichev, V. A. Yasakov, "Dvumernyye turbulentnyye techeniya reagiruyushchikh gazov" [Two-Dimensional Turbulent Flows of Reacting Gases], Novosibirsk, Nauka, 1976.

17. A. A. Stepanov, V. A. Shcheglov, Preprint, Lebedev Physics Institute, Moscow, 1976, No 182.

18. V. G. Krutova, A. N. Orayevskiy, A. A. Stepanov, V. A. Shcheglov, ZHURNAL TEKHNICHESKOY FIZIKI, Vol 47, 1977, p 2383.

19. Ya. Z. Virnik, V. G. Krutova, A. A. Stepanov, V. A. Shcheglov, KVANTOVAYA ELEKTRONIKA, Vol 4, 1977, p 2480.

20. V. G. Krutova, A. N. Orayevskiy, A. A. Stepanov, V. A. Shcheglov, KVANTOVAYA ELEKTRONIKA, Vol 3, 1976, p 1919.

21. U. Kh. Dorrens, "Giperzvukovyye techeniya vyazkogo gaza" [Hypersonic Viscous Gas Flows], Moscow, Mir, 1966.

22. Yu. V. Lapin, "Turbulentnyy pogranichenyy sloy v sverkhzvukovykh potokakh gaza [Turbulent Boundary Layer in Supersonic Gas Flows], Moscow, Nauka, 1970.

23. P. M. Chung, ADV. HEAT TRANSFER, Vol 2, 1965, p 110.

24. I. P. Ginzburg, "Treniye i teploperedacha pri dvizhenii smesi gazov" [Friction and Heat Transfer in Motion of a Gas Mixture], Leningrad, Leningrad State University, 1975.

25. A. N. Tikhonov, A. A. Samarskiy, "Uravneniya matematicheskoy fiziki" [Equations of Mathematical Physics], Moscow, Nauka, 1966.

26. A. A. Samarskiy, "Teoriya raznostnykh skhem" [Theory of Difference Schemes], Moscow, Nauka, 1977.

27. D. Potter, "Vychislitel'nyye metody v fizike" [Computational Methods in Physics], Moscow, Mir, 1975.

28. W. L. Shackleford, A. B. Witte, J. E. Broadwell, J. E. Trost, T. A. Jacobs, AIAA J., Vol 12, 1974, p 1009.

6610
CSO: 8144/1407

PHYSICS

UDC 535.375

INFLUENCE THAT SOME EMISSION PARAMETERS HAVE ON PUMPING WAVEFRONT REVERSAL IN A 'BRILLOUIN' MIRROR

Moscow KVANTOVAYA ELEKTRONIKA in Russian Vol 6, No 4(82), Apr 79 pp 765-771

[Article by N. G. Basov, V. F. Yefimkov, I. G. Zubarev, A. V. Kotov, A. B. Mironov, S. I. Mikhaylov and M. G. Smirnov, Physics Institute imeni P. N. Lebedev, Academy of Sciences USSR, Moscow]

[Text] An investigation is made of the influence that geometric, time and polarization characteristics of stimulating emission have on conditions of wavefront reversal (WFR) that accompanies stimulated Mandelstam-Brillouin scattering in various media. In a laser-amplifier arrangement almost total compensation is achieved for phase distortions of the laser signal that are introduced by amplifier elements. The output energy of the light beam in this case was 3 J, diameter 4 mm, divergence 0.3 mrad (diffraction divergence). The results of the experiments show the feasibility of practical application of WFR in high-power multichannel laser facilities.

1. At the present time there is a fairly widespread discussion in the literature concerning utilization of the WFR effect [Ref. 1-3] to compensate for static and dynamic inhomogeneities of the index of refraction in active media, as well as inaccuracies in alignment of elements in cascades of high-power optical amplifiers. The optimism of authors of some papers [Ref. 2, 3] is based on the results of successfully conducted experiments in WFR of ruby laser emission [Ref. 1, 2] with reflection from a "Brillouin" mirror. At the same time, in the actual circuits of powerful amplifiers the emission parameters may differ strongly from those used in demonstration experiments, which may appreciably disrupt the conditions of WFR (in particular our preliminary experiments on a high-power laser facility with a short (about 3 ns) pulse did not give unambiguous results). In our opinion, such significant differences include: 1) another active medium for lasers and amplifiers -- as a rule neodymium glass and the appreciable depolarization of radiation associated with the use of neodymium glass as the emission

passes through the amplification stages [Ref. 4]; 2) the unsteady nature of the process of stimulated Mandelstam-Brillouin scattering when pulses with duration $\tau \leq \tau_{ph}$ are used (τ_{ph} is the lifetime of an acoustic phonon); 3) the unsteadiness due to the effect of group delay of interacting fields when τ is of the order of L/c or less (L is the length of the cell); 4) strong saturation of amplifiers with reverse travel of the reflected pulse; 5) the use of multichannel amplifier circuits.

This paper is devoted to the experimental study of the influence that some of the above-mentioned factors have on the WFR process.

2. The experimental facility is shown in the diagram of Fig. 1. A pulse from master laser 1 passes through a two-power telescope and a Faraday decoupler, and is directed by a mirror and glass plate 6 to optical amplifier 7. The

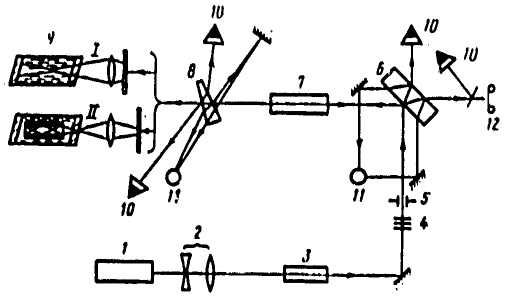

Fig. 1. Diagram of the experimental facility: 1--master laser; 2--two-power telescope; 3--Faraday decoupler; 4--attenuating filters; 5--diaphragms with diameter of 3-4 mm; 6--glass plate; 7--amplifier; 8--wedge; 9--systems for stimulating Mandelstam-Brillouin scattering; 10--calorimeters; 11--complex for measuring emission divergence; 12--camera

amplified radiation is used for pumping in "Brillouin" cell 9. After reverse travel through the amplifier, the reflected signal was coupled out of the system through plate 6.

The master laser was a standard neodymium glass unit with passive Q-switching and mode selection that operated under conditions close to single-mode lasing. The energy of the pulse introduced into the amplifier was from 0.1 to 5 mJ and was varied by filters. The duration of the pulse at half-height was about 25 ns when the spectral width $\Delta\nu$ was of the order of 0.005 cm^{-1} or less. The amplifier consisted of two stages with total weak-signal amplification of 50-100. Depolarization of emission as the signal traveled through the amplification stages did not occur as the beam being amplified traveled along the axis of the amplifier rods, and its size (d_b = 3-4 mm depending on the diameter of the output diaphragm) was much smaller than the diameter of the rods (d_r = 14 mm). WFR was achieved by using

either a system with focusing of pumping into the active medium of "Brillouin" cell 9 1, or a system with a light guide 9 11 (Fig. 1). The active medium in our experiments was acetone, CCl_4, gaseous SF_6 at a pressure of 22 atm, and K-8 glass in the system with focusing, and methane at a pressure of 150 atm and also carbon disulfide in the arrangement with the light guide.

The recording system provided for simultaneous measurement of the polar patterns of the radiation incident on and reflected from the "Brillouin" cell, the radiation of the master laser, and the radiation coupled out of the system. The corresponding energies were calorimetrically recorded. In addition, the intensity distribution of the output radiation was photographically recorded on I-1070 film at point 12 coupled to the output diaphragm of the master laser. Divergence was measured by a self-calibration method using mirror wedges and lenses with f = 2 m. The intensity distributions in the focal planes were photographed on I-1070 film. The reversal parameter -- the ratio of the reflected energy contained in an angle equal to the angle of divergence of the radiation incident on the cell, to the energy of the reflected signal incident on the aperture of the amplifier -- was determined by integrating the corresponding angular distributions of intensities in the incident and reflected signals. This parameter is a convenient quantity for characterizing the quality of WFR conditions.

The objects distorting the phase structure of the pumping wave in our experiments were: glass phase plates made by etching standard photographic plates in hydrofluoric acid (etching time 0.5-10 minutes), ruby rods of low optical quality, and also artificial turbulence of the atmosphere. Turbulence was set up by an ascending stream of hot air from a nichrome coil heated to about 700°C with a length of 100 cm, which was stretched out 10 cm below the axis of the pumping beam emanating from the amplifier. By using various phase-distorting objects and combinations, it was possible to change the "gray" divergence of the pumping radiation introduced into the Brillouin cell from 0.5 to 30 mrad (measured with respect to half-intensity level).

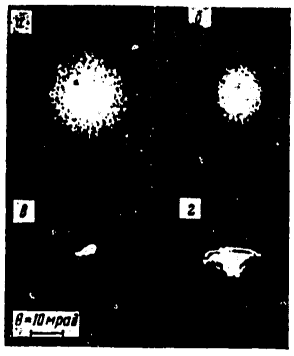

Fig. 2. Angular distribution of radiation after passing through phase-distorting objects: a, b--etched plate; c--artificial turbulence of the atmosphere; d--ruby rod

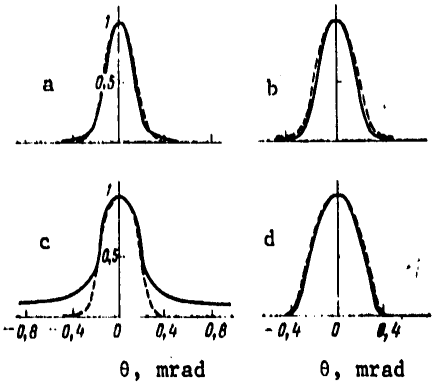

Fig. 3. Radiation patterns of input (broken line) and output (solid line) emission at the input to the amplifier (a), the output from the system (c), the input (b) and the output (d) from the cell with active medium with total reversal (a, b) and with incomplete reversal and strong saturation of the amplifier (c, d)

Shown in Fig. 2 as an example are photographs of the angular distribution of single-mode emission of a helium-neon laser ($\lambda = 632.8$ nm) after passing through some of the phase-distorting objects used in the experiment.

3. Shown in Fig. 3 are the radiation patterns of emission at the input to the amplifier and at the output from the system, as well as the emission incident on the cell and reflected from it. The system used for producing WFR was a light guide consisting of a glass tube 70 mm long with inside diameter of 3 mm filled with carbon disulfide. An image of the part of the phase plate illuminated by pumping was focused on the input end of the light guide by a lens with $f = 20$ cm. The phase plate increased the pumping divergence to $\theta \approx 15$ mrad. We can see that the amplifier has a certain detrimental influence on the divergence of the input signal close to the diffraction value, but this effect is canceled out in reverse travel. This shows that the reflected wave is reversed with respect to the pumping wave, i. e. the relation $E_{ref} = \text{const} \cdot E^*_{inc}$ is satisfied.

If the amplifier was operated in complete saturation, the unreversed component in the reflected signal, having a considerably broader polar pattern, traveled through sections of the amplifier rods with undepopulated inversion, and was amplified considerably better than the reversed component. This led to the occurrence of typical wings in the radiation pattern of the output signal if the intensity of the unreversed component was more than 1% of the intensity of the entire reflected signal. Fig. 3c, d illustrate just such a case: the unreversed component of the reflected signal cannot be seen on the radiation pattern of the emission emanating from the cell; however, because of strong saturation of the amplifier, effective "pulling" of the unreversed component takes place with respect to the reversed component. This negative effect can be easily eliminated in practice if the input aperture of the amplifier is matched to the diameter of the pumping beam. However, in our case this effect gave us an opportunity to increase the accuracy of determining the reversal parameter in the signal reflected from the cell. Depending on the phase-distorting object that was used, the

reversal parameter was 0.2-0.4 when the "gray" pumping divergence was 0.5-3 mrad, and increased to near unity for divergences of the order of 10 mrad or more, which agrees qualitatively with theoretical data [Ref. 5-7]. In experiments on wavefront reversal with focusing of pumping into the "Brillouin" cell, we were unable to observe any correlation of this kind between the gray divergence (within the range of our experiments $\theta_p/\theta_d \leq 100$) and the reversal parameter (disruption of WFR at a "gray" divergence of $\theta_p \sim 10^3\theta_d$ was observed in Ref. 8). After passing through the phase-distorting object, the initiating radiation was focused by a lens with a focal length of 10-15 cm into a cell 40 cm long filled with acetone or CCl_4. A typical peculiarity of the given mode of operation is that in the case of a space-limited angular pumping spectrum the reversal parameter was 0.6-0.9, while it fell off in the presence of wings to 0.1-0.3. This can be attributed to an increase in the transverse inhomogeneity of amplification at the focal pinch of the pumping beam in the second case [Ref. 8].

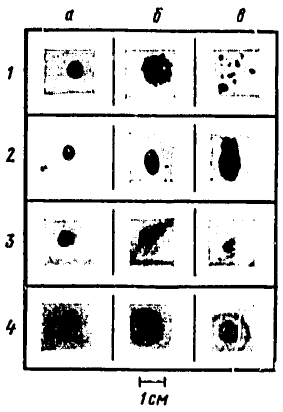

Fig. 4. Intensity distribution in the plane of the output diaphragm of the master laser

Another important characteristic of WFR along with the reversal parameter is the dimensions of the beam of reflected radiation; in realization of the reversal effect, these dimensions must coincide in any cross section with those of the beam of initiating radiation. Shown in Fig. 4 are photographs of the distribution of intensity of the reflected radiation after reverse travel of the amplification rods at a point in the plane of the output diaphragm of the master laser. Frame 1a corresponds to reflection from a "Brillouin" cell in the WFR mode; it can be seen that the beam dimensions coincide with those of the output diaphragm ($d_d = 4$ mm); frame 1b corresponds to reflection from an ordinary mirror placed in the location of the cell, and frame 1c -- to reflection from an ordinary mirror with a phase plate in front of it.

As we pointed out above, the "gray" divergence of pumping within the investigated limits has little influence on WFR in the version with focusing, and in particular one can convert to WFR even without predistortion of the wavefront of the initiating radiation. The WFR effect is observed for small values of intensity excess over pumping thresholds (Fig. 4, frame 2a), and gradually deteriorates as the intensity of the stimulating emission rises (Fig. 4, frames 2b, c). Let us note here that initially there is a halt to compensation of the astigmatism of the pumping beam due to focusing of the radiation into a cell with beveled windows. The reversal parameter was ~1 when focusing was done with short-focus lenses with f = 8-20 cm, and decreased with increasing f to 50-100 cm.

In the experiments described above, the scattering process was close to steady-state: for instance for CCl_4 $\tau_{pulse} \sim \tau_{settling} \approx \tau_{rise}\Gamma/2 \approx 15$-$20$ ns, where Γ is the gain increment. Therefore to determine the influence that scattering unsteadiness has on WFR conditions the gases that we used as the active media were SF_6 at $p = 22$ atm ($\tau_{rise} \sim 20$ ns) in the version with focused pumping, and methane at $p = 150$ atm ($\tau_{rise} \sim 17$ ns) in the version with scattering in a light guide. For these gases, the scattering conditions were quite unsteady: $\tau_{pulse} \sim {}^1/_{10}\tau_{settling}$. No deterioration of the WFR mode was observed.

It has been shown theoretically [Ref. 9] and experimentally [Ref. 10] that depolarization of initiating radiation leads to disruption of the wavefront reversal in a light guide. We investigated the influence that depolarization has on WFR in the arrangement with focusing of pumping. Used as the phase-distorting objects were ruby rods of poor optical quality (see for example Fig. 2d). At first the ruby rod was oriented with respect to the pumping polarization vector in such a way as to preclude polarization. When the emission emanating from the rod was focused into a cell with acetone, wavefront reversal was realized (Fig. 4, frame 3a). Then the ruby rod was turned about the longitudinal axis through 45°. When this was done, the state of polarization of the radiation at the output from the rod was strongly inhomogeneous over the cross section of the beam (the characteristic size of the inhomogeneity was about 0.5 mm). About 50% of the energy of the entire beam was contained integrally in each of two mutually perpendicular directions of the polarization vector. Shown in Fig. 4 (frames 3b, c) are photographs of the distribution of intensity of the output emission, frame 3c corresponding to a ruby rod of poorer optical quality than frame 3b. It can readily be seen that WFR conditions are sharply deteriorated with scattering of depolarized radiation in a "Brillouin" cell and in an arrangement with focusing of pumping.

In realizing WFR in a focused beam without predistortion of the phase structure of the initiating radiation, an appreciable part may be played by breakdown of the active medium in the cell due to the high intensities of the radiation in the focal pinch. In the given experiments the pumping radiation was focused by a lens with $f = 13$ cm into K-8 glass rods 6 cm long. When the pumping energy was changed from the breakdown threshold E_{br} to the threshold energy E_{th} of the stimulated Mandelstam-Brillouin scattering process, fracture traces 2-4 cm long were observed in the glass after passage of the laser pulse. When pumping exceeded the Mandelstam-Brillouin scattering threshold, the WFR process was observed (see Fig. 4, frame 4a). A further increase in pumping energy led to deterioration of WFR, which is apparently due to the fact that fractures in the active medium began to arise directly during the laser pulse (Fig. 4, frames 4b, c).

WFR of a multichannel beam may also have its own peculiarities due to the arbitrariness of the absolute phases of reflected signals. Shown in Fig. 5 is a setup that enabled us to simulate two-channel amplifier operation: the pumping beam was broken down into two parallel beams that were guided to the

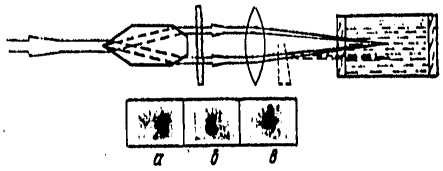

Fig. 5. Setup for studying WFR with multichannel excitation. Below are the distributions in the near zone for different modes of excitation of Mandelstam Brillouin scattering: one of the beams incident on the cell blocked (a); a glass wedge introduced into one of the beams (b); both beams focused in one place (c).

cell with the active medium upon passing through the phase plate. If both beams were focused onto the same spot of the cell, the phase structure of the pumping wave was reconstructed during reverse passage (Fig. 5 c). Independent scattering of the parallel channels in the cell could be realized by introducing an optical wedge into one channel. Then the reflected beams at the output of the splitting prism were incoherently added since their phases were not related. As a result, the structure of the intensity distribution of the output signal and also its radiation pattern varied from pulse to pulse depending on the realization of specific phase relations in the beams (see Fig. 5b). On the other hand when one of the beams was blocked (Fig. 5a) the divergence of the reflected radiation was twice that of the pumping divergence. This shows that insertion of amplitude distortions in the wave of initiating radiation is detrimental to reversal conditions.

4. The results of our experiments lead to the following conclusions.

a) Wavefront reversal permits effective compensation for the phase distortions of the master laser signal with reverse travel through the elements of the optical system. For instance in our experiments WFR was used to get a pulse with energy of about 3 J, duration of about 25 ns, beam diameter of about 4 mm and diffraction divergence (0.3 mrad).

b) It is experimentally found that the time unsteadiness of scattering with a change of "gray" divergence from 0.5 to 30 mrad has no effect on WFR conditions when $\tau_{pulse} \geq {}^{1}/_{10}\tau_{settling}$.

c) It is established that depolarization of initiating radiation is detrimental to WFR in standard systems (having in mind a system with focusing and a system with a light guide). In Ref. 10 we proposed and realized a system that gives wavefront reversal of depolarized radiation.

d) It is shown that to get diffraction divergence of the output radiation when the beam incident on the cell is split into two beams, it is necessary that these beams interfere in a "Brillouin" cell. This gives hope for coherent addition of the beams of multichannel systems.

REFERENCES

1. O. Yu. Nosach, V. I. Popovichev, V. V. Ragul'skiy, F. S. Fayzullov, PIS'MA V ZHURNAL EKSPERIMENTAL'NOY I TEORETICHESKOY FIZIKI, Vol 16, 1972, p 617

2. V. Wang, C. R. Giuliano, OPTICS. LETTS, Vol 2, 1978, p 4.

3. Yu. N. Kruzhilin, KVANTOVAYA ELEKTRONIKA, Vol 5, 1978, p 625.

4. N. G. Basov, P. G. Kryukov, Yu. V. Senatskiy, S. V. Chekalin, ZHURNAL EKSPERIMENTAL'NOY I TEORETICHESKOY FIZIKI, Vol 57, 1969, p 1175.

5. I. M. Bel'dyugin, M. G. Galushkin, Ye. M. Zemskov, V. I. Mandrosov, KVANTOVAYA ELEKTRONIKA, Vol 3, 1976, p 2467.

6. V. G. Sidorovich, ZHURNAL TEKHNICHESKOY FIZIKI, Vol 46, 1976, p 2168.

7. B. Ya. Zel'dovich, V. V. Shkunov, KVANTOVAYA ELEKTRONIKA, Vol 5, 1978, p 36.

8. V. I. Bespalov, A. A. Betin, G. A. Pasmanik, IZVESTIYA VUZov: SERIYA RADIOFIZIKA, Vol 20, 1977, p 791.

9. B. Ya. Zel'dovich, V. V. Shkunov, ZHURNAL EKSPERIMENTAL'NOY I TEORETICHESKOY FIZIKI, Vol 75, 1978, p 428.

10. N. G. Basov, V. F. Yefimkov, I. G. Zubarev, A. V. Kotov, S. I. Mikhaylov, M. G. Smirnov, PIS'MA V ZHURNAL EKSPERIMENTAL'NOY I TEORETICHESKOY FIZIKI, Vol 28, 1978, p 215.

6610
CSO: 8144/1407

PHYSICS

UDC 621.378.33

A CLOSED-CYCLE CW ELECTRON-BEAM-CONTROLLED CO_2 LASER

Moscow KVANTOVAYA ELEKTRONIKA in Russian Vol 6, No 4(82), Apr 79 pp 772-781

[Article by N. G. Basov, I. K. Babayev, V. A. Danilychev, M. D. Mikhaylov, V. K. Orlov, V. V. Savel'yev, V. G. Son and N. V. Cheburkin]

[Text] A cw electron-beam-controlled CO_2 laser is developed with regeneration of the gas mixture. The design gives emission on a wavelength of 10.6 μm with power of 10 kW and total efficiency of the installation of around 5%. The paper gives the results of an experimental study of the energy characteristics of a semi-self-maintained discharge in a CO_2-N_2-He-Xe-CO gas mixture under various combustion conditions. It is established that adding small amounts (about 1% by volume) of the gases Xe and CO to the gas mixture appreciably increases the limiting power of the semi-self-maintained discharge (by 30-50%), and correspondingly increases the lasing power and the efficiency of the installation. An analysis is made of the way that the output power of the laser depends on the pumping power, pressure, composition and flowrate of the gas mixture.

At the present time the electroionization method is one of the most promising for excitation of large volumes of dense active media in gas lasers in pulse [Ref. 1-4], quasi-cw [Ref. 6, 20] and cw [Ref. 5-7] modes of operation.

The solution of many scientific and technical problems (ranging and direction finding, communications, initiation of chemical reactions, machining and so forth) requires closed-cycle CO_2 lasers with high average power that is stable over a long period. Ref. 6 gives a brief description and the major characteristics of an electron-beam-controlled CO_2 laser (CO_2-EBL) with a closed cycle, and investigates the particulars of the semi-self-maintained discharge process at low electron beam densities under conditions of a closed gasdynamic loop.

An increase in the discharge volume as well as a number of design improvements have raised the output power and enabled prolonged stable operation of the

laser. This paper gives the principal results of an investigation of the characteristics of the first Soviet closed cycle cw CO_2-EBL.

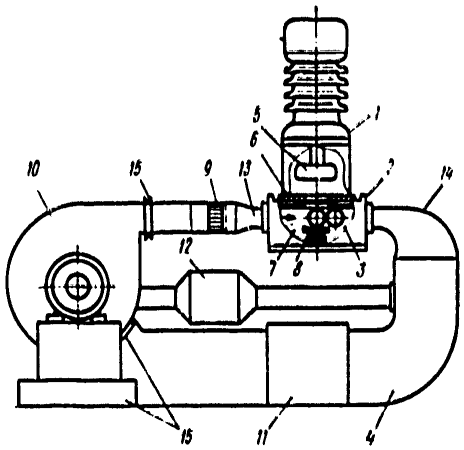

Fig. 1. Diagram of electron-beam-controlled laser

1. The CO_2-EBL (Fig. 1) consists of electron gun 1, discharge chamber 2, optical cavity 3, gasdynamic loop 4, electronic power supply systems and gas supply and evacuation systems (not shown in Fig. 1).

Triode electron gun 1 with beam size of 18 x 100 cm had straight-channel cathode 5 made up of eight tungsten filaments connected in parallel to a heater source. The accelerating voltage across the cathode of the gun was continuously controlled from 0 to 250 kV. Fluctuations of the cathode supply voltage did not exceed 2%, and pulsations of the accelerating voltage of the gun -- 5%. The residual pressure in the volume of gun 1 was maintained on a level of $2 \cdot 10^{-5}$ mm Hg. The electron beam was coupled into the discharge chamber through cooled aluminum foil 6 with thickness of 30 μm. The electron current was continuously controlled by varying the heater power for the tungsten filaments. The maximum density of electron current through the foil was 70 $\mu A/cm^2$, and the current density in the plane of the cathode of the discharge chamber was 10 $\mu A/cm^2$.

Nonuniformity of the current density of the central zone of the electron beam in the anode plane of the discharge chamber did not exceed 15%. When the accelerating voltage was changed from 210 to 120 kV, a 40% drop in the current density was observed in the anode plane of the discharge chamber. Stable continuous operation of the gun on a power level of 15 kW for several hours could be maintained by cooling the cathode and anode-foil units of the beam in combination with careful break-in conditioning.

The discharge cathode 7 was a cooled copper grid with geometric transparency of 70% located at a distance of 2 cm from the foil of the gun. Water-cooled

anode 8 was made up of two copper plates with a specially treated surface. A DC voltage of up to 5 kV with fluctuations not exceeding 5% was applied to the anode. The walls of the discharge chamber were shielded by dielectric plates. The distance between cathode and anode was 10 cm, the length of the discharge space along the optical axis was 100 cm, and the width along the flow was 20 cm.

Closed gasdynamic loop 4 was used to set up a uniform flow of the gas mixture through the discharge chamber. The parameters of the gasdynamic loop were calculated by conventional techniques [Ref. 17,18]. The gasdynamic loop included a centrifugal blower unit 10, water heat exchanger 11, regenerator 12, nozzle 13, exit cone 14, vibration couplings 15, and elements to direct and smooth out the velocity profile of the gas flow 9 (grids, cells). The rate of flow of the gas mixture through the discharge space was continuously regulated from 0 to 90 m/s by changing the rpm of the blower.

Nonuniformity of the field of velocities in the core of the flow was no worse than 10%. During electrical discharge in the discharge chamber the temperature at the chamber inlet increased from 20 to 40°C, and the flowrate remained practically unchanged. Catalytic regenerator 12 was used to maintain a stable level of stimulated emission without renewal of the gas mixture in the gasdynamic channel.

To increase the coefficient of utilization of the active medium, a three-pass unstable telescopic cavity was used with magnification of $M = 1.3$ composed of cooled copper mirrors. The overall length of the cavity was 5.42 m, and the radii [of curvature] of the convex and concave mirrors were 36 and 47 m respectively. The mirrors of the cavity were shifted 5 cm downstream relative to the electrodes of the discharge chamber. Special steps were taken to protect the mirrors from vibration of the elements of the loop. The laser emission was coupled out through a thermally stabilized NaCl window.

The directions of gas flow (arrow on Fig. 1), discharge field strength and the optical axis of the cavity resonator are mutually orthogonal. Emission power was recorded by a flow-through bolometer with signal registration by a loop oscilloscope. A standard calorimetric instrument was used for absolute calibration.

A central control panel was used to keep track of the working parameters of the individual subassemblies and to control the operation of the facility.

2. A semi-self-maintained discharge was struck in gas mixtures comprised mainly of CO_2, N_2 and He. The initial oxygen concentration did not exceed 0.1%. Under conditions of low electron-beam current densities, the power released in the cathode and anode zones is a significant fraction of the total electric power of the discharge. At pressures of about 50 mm Hg and "fast" electron current density j_e of the order of 10 $\mu A/cm^2$ or less, the anode-cathode potential drop is 20-30% of the total applied voltage, and hence the same ratio holds for the electric powers throughout the discharge and

anode-cathode zones. Typical current-voltage curves of a semi-self-maintained discharge are shown in Fig. 2.

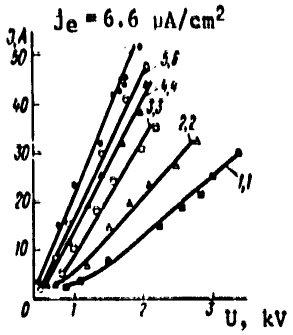

Fig. 2. Current-voltage characteristics of a semi-self-maintained discharge in a mixture of CO_2:N_2: He:Xe = 1:28:15:1 at a pressure of p = 46 mm Hg; flowrate v = 90 m/s, beam accelerating voltage U_b = 190 kV.

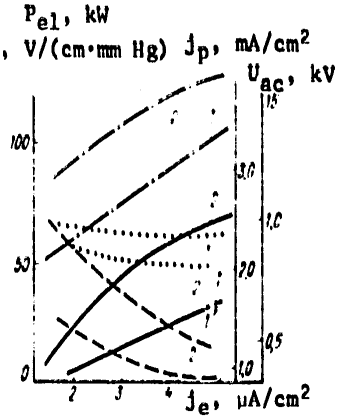

Fig. 3. Curves for discharge current density j_p (solid lines), anode-cathode potential drop U_{ac} (broken lines), electric power outside of the anode-cathode zones P_{el} (dot-and-dash lines) and the ratio E/p (dotted lines) as functions of the current density of "fast" electrons for mixtures: CO_2:N_2:He:Xe = 1:28:16:0 (1) and 1:28:16:0.6 (2); U_b = 180 kV, v = 90 m/s, p = 50 mm Hg

As a rule, the discharge current depended on the discharge voltage linearly at discharge current densities of at least 3-5 mA/cm². This enabled us to determine the anode-cathode potential drops by extrapolating the straight section of the current-voltage curve until it intersected the voltage axis. Direct determination of the voltage on the cathode layer gives a drop in this voltage as the discharge current density increases [Ref. 8]. However the drop is low (of the order of 100 V or less) practically throughout the entire region of discharge parameters typical for our experiments. This is confirmed by measurements of the anode-cathode potential drop on a model of the given facility using the method of varying the anode-cathode distance while maintaining other gas-discharge conditions [Ref. 6]. The values of the cathode potential drop found in this way are practically independent of the discharge current density and correspond within 10% to the simple graphic method of extrapolation. If the current-voltage characteristics had not been linear, and a power-law relation had held between the discharge current and the discharge voltage, the cathode potential drop could have been determined from the break in the current-voltage characteristic plotted in double logarithmic coordinates.

Shown in Fig. 3 is the cathode drop in potential as a function of the current density of "fast" electrons. With increasing electron current, the cathode potential drop decreases both in gas mixtures and in pure nitrogen. At the same time there is a reduction in the limiting discharge voltage at which a semi-self-maintained discharge is converted to an arc discharge. However, the total power and the discharge power outside of the cathode zone increase, as illustrated by Fig. 3. In this connection, the reduction in the cathode potential drop tends toward a constant value.

According to data of Ref. 5, the limiting energy input also saturates as the "fast" electron current increases. Thus it is advisable to use an external ionizer with current density of more than 20-30 $\mu A/cm^2$ even at pressures of about 200 mm Hg. Reduction of the external ionizer current to the optimum level leads to lower thermal loads on the extraction foil, a reduction in electron beam power, an increase in the overall efficiency of the laser facility and a reduction of accompanying x-ray emission.

For these reasons, current densities of the external ionizer of no more than 7 $\mu A/cm^2$ were used in the plane of the cathode of the discharge chamber. Let us note that at such a gun current density the energy input to the gas mixture is about 0.015 J/cm^3. This is only 20% below the energy input to the nitrogen and corresponds to the energy inputs to the gas mixture that are realized in discharge chambers of much smaller dimensions [Ref. 5].

It can be seen from Fig. 3 that doping the working mixture with up to 1% Xe when the current density of "fast" electrons is 1-2 $\mu A/cm^2$ enables a 40% reduction in the cathode voltage drop. This is most likely attributable to an increase in the total ionization cross section in the cathode zone. It is known that the ionization cross section of Xe in the region of electron energies from the ionization threshold to 100 eV is several times greater than the ionization cross section of CO_2, N_2 and He [Ref. 9]. As implied by the approximate theory of the cathode layer, the voltage drop near the cathode is inversely proportional to the total ionization cross section [Ref. 14, 15].

It has been established visually and photographically that the cathode layer is not homogeneous, but has a spotty structure. With an increase in discharge current there is an increase in the number of spots, and hence in the area of the plasma cathode. This fact is also noted in Ref. 8. By analogy with a self-maintained discharge, the increase in area of the plasma cathode as the discharge current rises, and the constant value of the anode-cathode potential drop over a broad range of discharge currents can be attributed to the existence of some constant "normal" current density for the given mixture and cathode material. In this connection, the beam of "fast" electrons ensures more or less uniform distribution of cathode spots over the cathode surface.

Let us also note that at "fast" electron current densities j_e of less than 3 $\mu A/cm^2$, fairly strong dependence of U_{ac} on j_e is observed (Fig. 3); at j_e of the order of 7-10 $\mu A/cm^2$ or more, U_{ac} is practically independent of j_e. Moreover, U_{ac} increases nearly linearly with increasing gas pressure.

It is known that the thickness of the cathode layer is a few Debye lengths. If the thickness of the layer is less than the mean free path of an electron determined by inelastic losses of energy in exciting vibrational and electronic degrees of freedom of molecules of N_2, CO_2, etc., an electron in the cathode field may acquire energy corresponding to the maximum value of the ionization function. If this is not the case, only a small fraction of the electrons emerging from the cathode will be able to acquire such energy, and a plasma cathode may not even arise at all. The ratio of the Debye length to the mean free path of an electron characterizes the energy losses of the electron in the cathode layer, and hence the cathode potential drop:

$$U_c \sim r_d \lambda^{-1} \sim \sigma_i N j_e^{-\frac{1}{2}}, \quad (1)$$

where σ_i is the effective cross section of inelastic collisions of an electron without consideration of ionization, cm^2; N is the total number of particles, cm^{-3}, j_e is the current density of high-energy electrons, r_d is the Debye radius in cm; λ is the mean free path, cm. Comparison with experimental data shows that relation (1) gives a qualitatively correct description of processes that take place in the cathode layer.

Let us also note that preceding the transition from a semi-self-maintained discharge to an arc, "spurts" appear on the cathode, streaming from individual cathode spots. The "spurts" do not cover the discharge gap, but apparently lead to an increase in discharge intensity in the zone of action due to the high conductivity of the plasma formed by ionized cathode metal vapor.

3. The dependence of discharge current density on "fast" electron current density (Fig. 3) is determined by process of ion-ion and electron-ion recombination, sticking and detachment of electrons. Estimates show that for the discharge conditions corresponding to Fig. 3, electron-ion recombination takes place with a constant k_{ei} close to $5 \cdot 10^{-8}$ cm^3/s, while sticking of electrons to CO_2 molecules is characterized by a constant k_a near 10^{-13} cm^3/s. In collisions of CO_2 with electrons, dissociation of CO_2 also occurs with a constant of k_d near 10^{-11}-10^{-12} cm^3/s, resulting in accumulation of O_2, CO and nitrogen oxides in the closed cycle. This leads to a change in time of both the discharge and lasing characteristics of the CO_2 laser.

In mixtures that contain CO_2, O_2 and nitrogen oxides, there is a reduction in discharge current as compared with the value determined by electron-ion recombination because of the appearance of negative ions in the reactions

$$CO_2 + e \rightarrow CO + O^-, \quad (2)$$

$$O_2 + e \rightarrow O + O^-, \quad (3)$$

$$CO_2 + O^- + M \rightarrow CO_3^- + M, \quad (4)$$

$$N_2O + e + M \rightarrow N_2O^- + M. \quad (5)$$

As shown in Ref. 10, the concentration of negative ions in the gas flowing through a discharge gap of about 1 cm at a rate of 100 m/s may reach values comparable to the electron concentration.

The use of a catalytic regenerator in which product gases O_2 and CO are combined into carbon dioxide gives stable discharge characteristics. This is shown in Fig. 4 which gives the change in voltage-power characteristics of a discharge with elapsed time and stabilization of these characteristics when a catalytic regenerator is included.

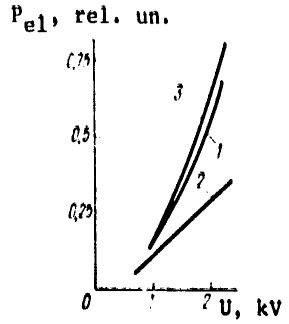

Fig. 4. Voltage-power characteristics of a semi-self-maintained discharge in a gas mixture of CO_2, N_2, He and Xe: 1--initial, 2--after 10 minutes of operation with two arc, 3--after 15 minutes of operation with seven arcs

As demonstrated in Ref. 11, the plasma conductivity can be increased by adding CO that promotes destruction of negative ions in the reactions

$$O^- + CO \rightarrow CO_2 + e, \qquad (6)$$

$$CO_3^- + CO \rightarrow 2CO_2 + e. \qquad (7)$$

For instance adding carbon monoxide in an amount of 0.5-1.5 mm Hg to a mixture of CO_2:N_2:He = 1:30:15 mm Hg increases conductivity with an operating regenerator by 20-30%. The cathode drop in this case does not change. It should be noted that the addition of CO to a gas mixture that contains a few percent of oxygen may nearly double conductivity. Besides, when a catalytic regenerator is in operation there will be a reduction in the amount of oxygen in the mixture to the point of total disappearance for the corresponding concentrations of O_2 and CO.

The presence of 1-5% Xe in the gas mixture not only reduces the cathode potential drop, but also leads to an increase of discharge current and maximum power inputs as shown in Fig. 2 and 3. A considerable change of plasma conductivity is observed only when Xe is added in amounts of less than 1% of the total pressure of the mixture. A further increase in the partial pressure of Xe to 5% only weakly increases the plasma conductivity, while the limiting voltage of the semi-self-maintained discharge and accordingly the electric power decrease.

There are several possible explanations of this effect. In the first place there is an increase in the degree of ionization of the mixture by "fast" electrons since there is an increase in the average nuclear charge of the gas mixture. However, this could hardly lead to an increase of conductivity by more than 5%.

In the second place, the electron concentration increases as a result of direct or step-by-step ionization of Xe in the discharge. Estimates of the rate of direct ionization of Xe in the discharge assuming maxwellian energy distribution of electrons with temperature $T_e = 0.7$ eV (the electron concentration evaluated from plasma conductivity is $n_e = 10^{11}$ cm^{-3}, the electron energy dependence of the ionization cross section is taken from Ref. 9) show that the rate of semi-self-maintained ionization (10^{13}-10^{14} cm^3/s) is comparable to that of self-maintained ionization at a xenon partial pressure of the order of 1 mm Hg. It is also known that maxwellian distribution of electrons is less rich in "fast" electrons than the actual distribution for mixtures of CO_2-N_2-He at the same effective temperature. It should be noted that in addition to direct ionization of Xe, a process of step-by-step ionization is possible through a metastable level of Xe with energy 8.32 eV that is populated in the discharge in collisions with both electrons and metastable N_2 molecules.

In the third place, The excited Xe atoms may increase the rate of destruction of negative ions in the discharge. This is possible only in the case where this process has a constant of about 10^{-7} cm^3/s, since according to the data of Ref. 12 the destruction of negative ions by excited nitrogen takes place with a constant of about 10^{-9} cm^3/s, and the amount of nitrogen in the mixture exceeds the amount of xenon by a factor of nearly 100.

The two latter processes should lead to a reduction in the voltage threshold of discharge stability [Ref. 5, 13]. In particular, in the second case, ionization instability may develop due to a sharp increase in electron concentration as excited xenon atoms are ionized. Since the threshold of step-by-step ionization is lower for Xe than for N_2, instability develops at lower electric field strengths. This is observed experimentally as well (see Fig. 4).

The enumerated processes can be attributed to saturation of conductivity as a result of an increase in the amount of Xe. In the second case this occurs due to a reduction in the number of "fast" electrons in the presence of Xe, while in the third case it is due to the total disappearance of negative ions.

4. Shown in Fig. 5 are curves for the limiting input powers (to the zone outside of the cathode) as a function of composition, pressure and flowrate of the gas through the discharge gap. The limiting power is determined by the voltage and the corresponding discharge current at which uniform burning stops and the discharge becomes an arc.

The limiting power of the discharge increases linearly with an increase in the rate at which the gas mixture is pumped through. The installation provided a gas flowrate in the core of the stream of $v = 90$ m/s in the discharge channel. At these gas flowrates, the ratio of the electric power of the blower motors to the electric power of the discharge is of the order of 0.1-0.15. Since the discharge power increases in proportion to v, while the electric power consumed in moving the gas in the gasdynamic loop is

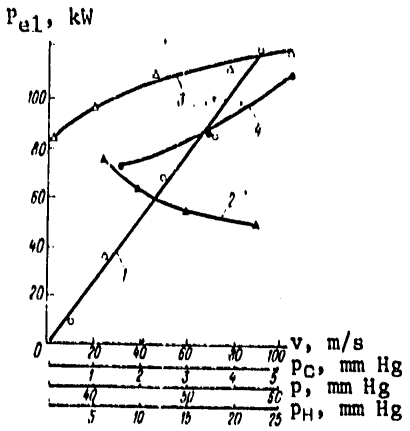

Fig. 5. Curves for the limiting electric power P_{el} outside of the anode-cathode zones as a function of flowrate v (1), partial pressures of carbon dioxide p_C (2) and helium p_H (3), and total pressure p (4): 1--CO_2:N_2:He:Xe:CO = 1:31:16:0.8:1, p = 50 mm Hg; 2--CO_2:N_2:He:Xe = (p_C/1.1):30:16:1, p - p_C = 48 mm Hg; 3--CO_2:N_2:He:Xe = 1:21.5:(p_H/1.7):1, p - p_H = 40 mm Hg; 4--CO_2:N_2:He:Xe = 1:30:16:0.6; v = 90 m/s (2-4); U_b = 180 kV; j_e = 6.5 μA/cm^2

proportional to v^3, from the standpoint of efficiency of the installation it is advisable to increase the flowrate past 150 m/s.

An increase in the partial pressure of CO_2 in a mixture with N_2, He and Xe leads to a reduction in the maximum power of the electric discharge. In this case there is a drop in the limiting voltage of the discharge (apparently due to the development of instabilities caused by the presence of a large number of negative ions [Ref. 5, 13]. In addition, due to the sticking processes described by reactions (2)-(5) there is a reduction of plasma conductivity.

There is an increase in the limiting electric power with rising total gas pressure of the mixture (Ref. 5). But at the same time, the limiting value of E/p falls off (E is the limiting electric field strength in V/cm; p is the initial overall pressure in mm Hg). This fact is analogous to the reduction of breakdown values of E/p as the value of pd increases (d is the length of the discharge gap) at low levels of semi-self-maintained ionization (Paschen curve) [Ref. 16]. In a qualitative sense, the same relations show up as the pressure of the mixture is increased by adding helium.

5. The lasing power increases linearly as the input power is raised (Fig. 6). In this connection, as the total pressure of the mixture is increased there is a reduction in the efficiency of stimulated emission, since when the transparency of the optical cavity is fixed, its efficiency falls off with increasing pressure and hence with a reduction in gain.

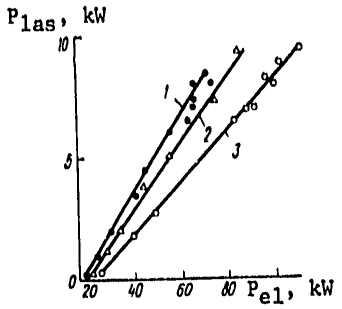

Fig. 6. Curves for lasing power as a function of electric power outside of the anode-cathode zones for a mixture of CO_2:N_2:He:Xe = 1:30:16:0.6 at a pressure of p = 42 (1), 52 (2) and 61 mm Hg (3); U_b = 180 kV, j_e = 6.5 μA/cm^2, v = 90 m/s.

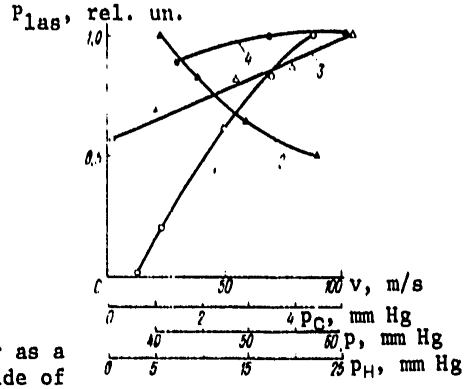

Fig. 7. Curves for lasing power as a function of limiting electric power outside of the anode-cathode zone. Conditions and notation on Fig. 5.

As has already been pointed out, an increase in the pumping rate of the gas mixture enables an increase in the limiting electric power, and accordingly in the lasing power (Fig. 7). At high flowrates there is an decrease in the pace at which the lasing power increases, which can be attributed to the influence of processes of transport of excited molecules of CO_2 and N_2 out of the resonator.

With increasing partial pressure of CO_2, there is a reduction of efficiency as well as lasing power. This is apparently due to an increase in the population of the lower laser level and a reduction in the fraction of energy expended in excitation of the 00^0v mode of CO_2 molecules and vibrations of N_2 molecules.

With increasing absolute pressure of He in the mixture there is an increase in the rate of de-excitation of the lower laser level and a rise in lasing power (Ref. 7). Let us note the rather high efficiency (about 5%) of a laser with a mixture that does not contain He.

6. The given parameters and characteristics of the laser correspond to gun accelerating voltages of 180-190 kV. Such a voltage combined with the low densities of "fast" electron current sharply reduces the loads on the aluminum foil at the gun output.

Operation of the beam at an accelerating voltage of 100-200 kV enables a reduction in overall dimensions and simplifies the design of the gun and power supply sources, and also reduces the accompanying x-radiation by a considerable factor. Besides, a reduction in "fast" electron energy results in increased ionization of the gas mixture in the discharge chamber.

Careful break-in conditioning of the gun made it possible to operate continuously (for about an hour) at an accelerating voltage of 120 kV. It was established that at the same gun current the discharge current increases by a factor of 1.3 with practically constant limiting discharge power, while the ratio of gun power to electric discharge power is cut in half.

7. The distribution of laser emission intensity in the far zone (at the focus of the mirror with radius of 30 m) was studied by an optical knife cutting the focal spot at a rate of 7.5 mm/s [Ref. 19]. The emission power reflected from the optical knife was recorded by a flow-through bolometer and a loop oscilloscope.

Analysis of measurement results gave a laser radiation divergence (angle between the optical axis of the bean and the generatrix of the pencil of rays including 80% of the emission power) equal to $(5-7)\cdot10^{-4}$ rad.

8. The experiments that were done demonstrate the effectiveness of using the electroionization method of pumping for excitation of cw CO_2 lasers. The energy inputs attained by the electroionization method on a level of 0.019 J/cm^3 (300 kJ/kg) in large discharge volumes (~10^4 cm^3) result in a rather high level of stimulated emission. The addition of small amounts of Xe (~1%) to the working mixture of a CO_2 laser increases the maximum energy parameters of the facility.

The use of a catalytic regenerator and small additions of CO in the gas mixture of a CO_2 laser enable prolonged operation of a closed-cycle laser without changing the gas mixture. In this connection, high purity of the initial gases with respect to oxygen is not an absolute necessity.

The results lead us to hope for extensive application of closed-cycle CO_2-EBL's.

In conclusion the authors express their deep gratitude to G. G. Dolgov-Savel'yev for useful discussion of the results, to A. P. Dzisyak, A. I. Lazurchenkov and Z. I. Ashurly for taking part in developing the regenerator, and also to V. I. Ivanov, V. N. Lisov, B. P. Malugin, A. I. Tishchenko and A. A. Kholodilov for assisting with the experiments.

REFERENCES

1. N. G. Basov, E. M. Belenov, V. A. Danilychev, O. M. Kerimov, I. B. Kovsh, A. F. Suchkov, PIS'MA V ZHURNAL EKSPERIMENTAL'NOY I TEORETICHESKOY FIZIKI, Vol 14, 1971, p 421.

2. S. A. Fenstermacher, M. J. Nutter, J. P. Rink, K. Boyer, BULL. AMER. PHYS. SOC., Vol 16, 1971, p 42.

3. J. D. Dugherty, E. R. Pugh, D. H. Douglas-Hamilton, BULL. AMER. PHYS. SOC., Vol 17, 1972, p 399.

4. N. G. Basov, V. A. Danilychev, A. A. Ponin, I. B. Kovsh, V. N. Sobolev, ZHURNAL TEKHNICHESKOY FIZIKI, Vol 43, 1973, p 2357.

5. Ye. P. Velikhov, S. A. Golubev, A. S. Kovalev, I. G. Persiantsev, V. D. Pis'mennyy, A. T. Rakhimov, T. V. Rakhimova, FIZIKA PLAZMY, Vol 1, 1975, p 847.

6. A. V. Anokhin, I. K. Babayev, N. A. Blinov, A. F. Grachev, D. G. Dolgov-Savel'yev, M. D. Mikhaylov, V. K. Orlov, V. F. Razumtsev, V. V. Savel'yev, N. V. Cheburkin, KVANTOVAYA ELEKTRONIKA, Vol 2, 1975, p 211.

7. E. Hoag, H. Pease, J. Staal, J. Zar, APPL. OPTICS, Vol 13, 1974, p 1959.

8. S. A. Golubev, A. S. Kovalev, N. A. Loginov, V. D. Pis'mennyy, A. T. Rakhimov, FIZIKA PLAZMY, Vol 3, 1977, p 1011.

9. D. Rapp, P. Englander-Golden, J. CHEM. PHYS., Vol 43, 1965, p 1464.

10. W. J. Wiegand, W. L. Nighan, APPL. PHYS. LETTS., Vol 22, 1973, p 583.

11. H. Shields, A. L. Smith, B. Norris, J. PHYS. D: APPL. PHYS., Vol 9, 1976, p 1587.

12. J. L. Mouruzzi, D. A. Price, J. PHYS. D: APPL. PHYS., Vol 7, 1974, p 1434.

13. A. P. Napartovich, A. N. Starostin, FIZIKA PLAZMY, Vol 2, 1976, p 843.

14. V. A. Granovskiy, "Elektricheskiy tok v gaze" [Electric Current in Gas], Moscow, Nauka, 1971.

15. N. G. Basov, E. M. Belenov, V. A. Danilychev, O. M. Kerimov, I. B. Kovsh, A. F. Suchkov, ZHURNAL TEKHNICHESKOY FIZIKI, Vol 62, 1972, p 2540.

16. E. D. Dozanskiy, O. B. Firsov, "Teoriya iskry" [Spark Theory], Moscow, Atomizdat, 1975.

17. I. Ye. Idel'chik, "Spravochnik po gidravlicheskim soprotivleniyem" [Handbook on Hydraulic Drag], Moscow, State Power Engineering Press (GEI), 1960.

18. S. M. Gorlin, N. I. Slezinger, "Aeromekhanicheskiye izmereniya. Metody i pribory" [Aeromechanical Measurements. Methods and Instruments], Moscow, Nauka, 1964.

19. D. R. Stinner, R. E. J. Witcher, J. PHYS. ENG., Vol 5, No 3, 1972, p 237.

20. Ye. P. Velikhov, Yu. K. Zemtsov, A. S. Kovalev, I. G. Persiantsev, V. D. Pis'mennyy, A. T. Rakhimov, ZHURNAL EKSPERIMENTAL'NOY I TEORETICHESKOY FIZIKI, Vol 67, 1974, p 1682.

6610
CSO: 8144/1407

PHYSICS

UDC 621.378.325

STIMULATED EMISSION OF MICROSECOND PULSES IN A RING LASER

Moscow KVANTOVAYA ELEKTRONIKA in Russian Vol 6, No 4(82), Apr 79 pp 851-852

[Article by V. V. Arsen'yev, T. N. Matveyev, A. N. Stepanov and N. D. Ustinov]

[Text] The paper describes a solid-state ring laser in which square pulses of microsecond duration are produced by using an electro-optical feedback loop and a special law for Q-switching the cavity. To compensate for delay of the feedback signal, the laser utilizes matching of the light-pulse travel time around the cavity half-ring with the electric pulse time of travel through the feedback circuit, which eliminates the spike on the emission pulse front and reduces fluctuations of emission on its peak. The use of a traveling-wave lasing mode made it possible to get stable microsecond square pulses with a low number of transverse modes, as well as reducing the divergence of emission to 3-4'.

One of the most effective ways to increase the emission pulse length of solid-state lasers with Q-switching to a microsecond or more is to use electro-optical negative feedback (NFB) and a special law for Q-switching the cavity [Ref. 1-3]. However, the pulses produced by this technique have

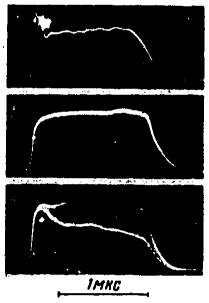

Fig. 1

considerable fluctuations at the peak (Fig. 1a). These fluctuations were least noticeable in a cavity with configuration close to semiconcentric with a large number of stimulated transverse modes [Ref. 1].

A considerable disadvantage of lasers with such a configuration of the cavity is the large divergence of radiation, exceeding 30'. Attempts to reduce the divergence by reducing the number of modes lead to an increase in the fluctuations on the pulse peak and a reduction in pulse stability. Besides, in these lasers there is a sharp lasing spike on the emission pulse front even with stimulated emission of microsecond pulses that have a smooth peak. This spike is due to delay of the NFB signal in the electric circuit by a time τ_d relative to the instant of arrival of the light wave that causes this signal at the light shutter. Complexity in eliminating the influence of signal delay in the NFB circuit is due to the fact that the minimum length of the NFB circuit as dictated by the lengths of the photocell and coupling cable is 30-40 cm. Besides, the light shutter simultaneously transmits both the forward and reverse waves, the feedback signal acting on each of these, so that delay of the NFB signal is compensated only for a wave in one direction.

In this paper we propose a laser with electro-optical feedback in which the influence of delay of the electric NFB signal with respect to the corresponding light wave is eliminated by using a ring cavity operating in the traveling wave mode. In such a resonator one can match the times of arrival of the feedback signal and the corresponding light wave at the light shutter, and hence eliminate the cause of the spike on the pulse front. Moreover, the traveling wave mode eliminates competition of traveling waves of the cavity, and consequently obviates the need for using a large number of transverse modes to form a smooth peak on the microsecond pulse, which is important in reducing emission divergence.

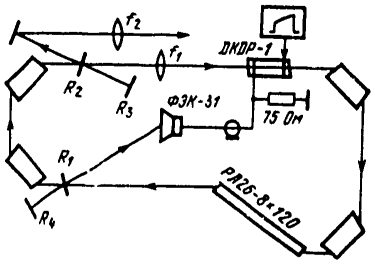

Fig. 2

Research was done on a ruby laser shown schematically in Fig. 2. The cavity was formed by 90° Brewster prisms. The NFB signal was taken off from coaxial photocell ФЭК-31 to which part of the radiation of the cavity was diverted by a semi-transparent dielectric mirror with reflectivity $R_1 = 0.3$. The times of arrival of the light wave and NFB signal at the shutter were matched by

changing the length l of the part of the cavity from mirror R_1 to the shutter when mirror R_1 is displaced along the axis of the cavity, or by changing the signal delay τ_1 in the NFB circuit when the length of the coupling cable is increased. Q-switching of the cavity was accomplished with crystal DKDP-1 [dipotassium orthophosphate] with simultaneous application of the modulating voltage pulse formed in accordance with a special law and the NFB signal. The emission was coupled out of the cavity by a dielectric mirror with $R_2 = 0.3$ set at an angle of 5-10° to the axis of the cavity. To get a traveling wave, a passive valve was used based on reflecting mirrors with $R_3 = R_4 = 0.99$. A state close to single-mode operation was attained by introducing a positive lens into the cavity with focal length $f_1 = 1$ m, and by adjusting it to confocal configuration.

Mirror R_1 was moved to satisfy the relation $\tau_d = \tau_1 - l/c = 0$, resulting in shaping of smooth microsecond pulses without a spike on the wavefront. The resultant pulses (Fig. 1b) retained their shape with displacement of the mirror R_1 along the cavity axis over a range of $\Delta l \approx \pm 10$ cm. With a further increase in τ_d (Δl), regular oscillations appeared on the pulse peak with frequency $1/T \approx 120$-360 MHz (Fig. 1c).

A change in the configuration of a spherical cavity in the range $0 < L/f < 4$ did not have such an appreciable effect on pulse shape as in the two-mirror cavity [Ref. 1]. In the case of the confocal configuration most frequently used in practice, stable lasing with a microsecond pulse close to single-mode was achieved. This shows that in a ring cavity the stability of the peak of a microsecond pulse depends less on the number of transverse modes than in a two-mirror cavity.

The emission divergence attained after correction with a lens having $f_2 = 2$ m was about 3-4' at a pulse recurrence rate of 1-3 Hz. The spectral width of the radiation was 0.05-0.1 Å. Corresponding to such a wide laser radiation line are a large number of axial modes, which reduces modulation of the pulse peak due to beats. Moreover, to reduce fluctuations on the pulse peak, maximum inhomogeneity of the field along the axis was set up in the active element by locating this element close to the pinch produced by lens f_1.

Thus the use of a ring laser with electro-optical NFB makes it possible to shape microsecond square pulses with a smooth peak without a spike on the leading edge with small emission divergence.

REFERENCES

1. V. V. Arsen'yev, V. N. Lomakin, I. N. Matveyev, A. N. Stepanov, KVANTOVAYA ELEKTRONIKA, Vol 3, 1976, p 1035.

2. R. V. Lovberg, E. R. Wooding, M. L. Yeoman, IEEE J., QE-11, 1975, p 17.

3. V. V. Arsen'yev, I. N. Matveyev, Yu. V. Prichko, A. N. Stepanov, PRIBORY I TEKHNIKA EKSPERIMENTA, No 2, 1976, p 158.

6610
CSO: 8144/1407

PHYSICS

UDC 535.36:538.3

CONCERNING IMPRECISION IN THE REPRODUCTION OF THE SPATIAL STRUCTURE OF A BEAM IN THE AMPLIFYING MEDIUM OF LASER SYSTEMS WITH A REVERSING MIRROR

Moscow KVANTOVAYA ELEKTRONIKA in Russian Vol 6, No 4(82), Apr 79 pp 864-867

[Article by G. G. Kochemasov and V. D. Nikolayev]

[Text] An examination is made of the influence that inhomogeneities of gain and refractive index in the active medium of a two-pass amplifier with ideal wavefront-reversing mirror have on the accuracy of reproduction of spatial distributions of the amplitude and phase of the input signal. It is shown that in the case where inhomogeneities of the index of refraction are fairly small and the amplifier can be treated as a thin lens (phase corrector), the wavefront of the output radiation is reversed with respect to the wavefront of the input signal. Otherwise reversal does not occur.

The effect of wavefront reversal is being more and more extensively used in the process of stimulated scattering. It was shown for the first time in Ref. 1 that when certain conditions are met the field of the Stokes component of stimulated Mandelstam-Brillouin scattering is complex-conjugate to the pumping field. Wavefront reversal can be realized in other nonlinear processes as well [Ref. 2-5] and has various applications (see for instance Ref. 6-8).

In all arrangements a beam with a certain spatial structure (in the form of a flat wave [Ref. 6] or radiation scattered from a target [Ref. 7, 8] passes through an amplifier, is reflected from a wavefront reversing "mirror" and passes a second time through the amplifying medium. In accordance with the principle of reversibility, it is assumed that the field of the output radiation of such a two-pass amplifier is complex-conjugate to the field of the input signal.

However, it is clear that in an inhomogeneous amplifying medium the principle of reversibility is only approximately valid. In this paper we examine how

this situation affects the accuracy of reproduction of the spatial structure of the input signal in a two-pass amplifier. Actually, the equations that describe propagation of laser emission in an amplifying medium

$$\frac{\partial E_1}{\partial z} = \frac{i}{2k}\Delta_\perp E_1 + ik\delta n(r)E_1 + \frac{(\alpha-\varkappa)}{2}E_1,$$
$$-\frac{\partial E_2}{\partial z} = \frac{i}{2k}\Delta_\perp E_2 + ik\delta n(r)E_2 + \frac{(\alpha-\varkappa)}{2}E_2, \qquad (1)$$

are not complex-conjugate when $\frac{d}{dr}(\alpha-\varkappa)\neq 0$. In (1), $E_{1,2}$ are the complex amplitudes of the forward and reverse waves; k is the wave number, $\Delta_\perp$ is the Laplace operator with respect to transverse coordinates, α and $\varkappa$ are the coefficients of amplification and absorption, $\delta n(r)$ is the inhomogeneous component of the index of refraction. If amplification and absorption are homogeneous, then after substitution of variables $\tilde{E}_{1,2}=E_{1,2}\exp[\pm\frac{1}{2}(\alpha-\varkappa)z]$ equations (1) become complex-conjugate. In such a medium the principle of reversibility for rays becomes valid.

As implied by (1), the presence of transverse nonhomogeneities of amplification or absorption leads to violation of the principle of reversibility and to imprecision of reproduction. We illustrate this by the example of a lens-like medium in the state of linear amplification:

$$\delta n(r)=\Delta n(r/a)^2;$$
$$\alpha(r)=\alpha_0[1-(r/b)^2],\quad \varkappa=0. \qquad (2)$$

We take the input signal of the amplifier as gaussian, and assume that the reversing mirror is ideal. It is known [Ref. 9] that during propagation in a lens-like medium, such a beam remains gaussian and for describing it one can conveniently use a matrix method. Using this method, we introduce the parameter

$$\frac{1}{q(z)}=\frac{1}{R(z)}-i\frac{2}{kw^2(z)}, \qquad (3)$$

where R(z) is the radius of curvature of the wavefront, w(z) is the transverse dimension of the beam. The value of $q_1(l)$ after a single passage through the amplifier is related to the parameter of the input signal $q_1(0)$ by the expression

$$q_1(l)=\frac{Aq_1(0)+B}{Cq_1(0)+D}, \qquad (4)$$

where A, B, C, D are the elements of the transfer matrix. In the case of a lens-like medium of length l,

$$A=D=\cos\sqrt{n_2}l;\quad B=-\frac{C}{n_2}=-\frac{1}{\sqrt{n_2}}\sin\sqrt{n_2}l,$$
$$n_2=-\frac{2\Delta n}{a^2}+i\frac{\alpha_0}{kb^2};\quad \sqrt{n_2}l\quad x+iy\approx\frac{\alpha_0 al}{2kb^2\sqrt{2\Delta n}}+i\frac{\sqrt{2\Delta n}\,l}{a};\quad x\ll y.$$

Here for the sake of definiteness we consider a defocusing medium. The transformation realized by the reversing mirror can be represented as

$$q_2(l) = q_1^*(l). \qquad (5)$$

Relations (4) and (5) are sufficient for determining the parameter $q_2(0)$ at the output of the two-pass amplifier:

$$\frac{1}{q_2(0)} = -\frac{1}{R_2(0)} + \frac{i2}{kw^2(0)} = \frac{\frac{1}{q_1^*(0)}(AA^* + n_2BB^*) + (n_2BA^* - n_2^*B^*A)}{\frac{1}{q_1^*(0)}(AB^* - A^*B) + (AA^* + n_2^*BB^*)}. \qquad (6)$$

In the general case expression (6) is too cumbersome. Therefore let us consider the limiting cases that are of the greatest interest.

A thin lens: $x \ll y \ll 1$. With accuracy to a quantity of the second order of smallness with respect to x, we find that the values of the radii of curvature of the wavefronts of the output radiation and the input signal coincide, and the transverse dimension of the beam becomes less:

$$w_{вых} = \frac{w_{вх}}{\sqrt{1 + 2\alpha_0 l w_{вх}^2 b^2}}. \qquad (7)$$

[note subscripts вх = input, вых = output]. This result has a simple meaning, and can be obtained from the following considerations. In the thin-lens approximation the beam trajectories can be taken as rectilinear, and the influence of inhomogeneities can be accounted for as phase advances and amplification along the trajectories. The inhomogeneous phase lead in a thin lens is compensated in reverse travel through the medium. To find the distribution of intensity in the cross section at the amplifier output, and hence to find $w_{вых}$ it is sufficient to write

$$I_{вых}(r) = I_{вх}(r)e^{2\alpha(r)l} = I_{вых}(0)e^{-(r/w_{вых})^2}.$$

In this case we arrive again at formula (7). It is clear that in an optically thin amplifier with arbitrary (and not only lens-like) medium, wavefront reversal and beam constriction will take place. Under conditions of amplification saturation the effect of constriction will be less pronounced and the degree of constriction will depend on the length of the unsaturated section of the active medium.

A thick lens: $x \ll 1$, $y \geq 1$, i. e.

$$l \geq a/\sqrt{2\Delta n} = l_{пр}, \qquad (8)$$

($l_{пр}$ is the limiting length). In the case of an input signal in the form of a planar wave

$$R_{вых} = a/\sqrt{2\Delta n}, \quad w_{вых} = 2b\sqrt{2\Delta n}/\sqrt{\alpha_0 l}. \qquad (9)$$

i. e. reproduction is absent. The beam parameters (9) correspond to the fundamental mode of an active waveguide (2). In reality at a distance $l \geq l_{пр}$ the fundamental waveguide mode is isolated so that the beam practically "forgets" its initial structure. From the standpoint of geometric optics, the quantity $l_{пр}$ corresponds to the distance within which a ray parallel to the

optical axis will cross the active region and go beyond its limits. Obviously under saturation conditions the radius of curvature of the wavefront will not change, and the beam size will increase to about b. In this case the divergence at the amplifier output will be $\theta_{вых} = (2b/a)\sqrt{2\Lambda n}$, and will coincide with the divergence in lasers with an inhomogeneous active medium and a plane-parallel cavity [Ref. 10].

The reason for the lack of reversal of the wavefront in a thick distributed lens is that the propagation of a reversed convergent wave is unstable, and the perturbations caused by gain inhomogeneity are sufficient to convert this wave to a diverging wave. We can convince ourselves of this if we use a relation of type (4) for the reverse wave and postulate $l > l_{пр}$, $a_0 = 0$ and $q_2(l) = -q_1(l) + \delta q$. When $\delta q = 0$, we have $q_2(0) = -q_1(0)$, i. e. exact reversal takes place. In the presence of perturbations ($\delta q \neq 0$) such a length $l > l_{пр}$ eixsts that the radius of curvature after reverse travel through an inhomogeneous medium is equal to $-l_{пр}$. In the amplifier the gain inhomogeneities play the part of such perturbations.

Thus the gain inhomogeneities in the medium impose fundamental limitations on the accuracy of reproduction of the wavefront in lasers with a reversing mirror. Effective dynamic compensation of aberrations is possible only in amplifiers in which the active media can be considered thin lenses.

REFERENCES

1. B. Ya. Zel'dovich, V. I. Popovichev, V. V. Ragul'skiy, F. S. Fayzullov, PIS'MA V ZHURNAL EKSPERIMENTAL'NOY I TEORETICHESKOY FIZIKI, Vol 15, 1972, p 160.

2. B. Ya. Zel'dovich, N. A. Mel'nikov, N. F. Pilipetskiy, V. V. Ragul'skiy, PIS'MA V ZHURNAL EKSPERIMENTAL'NOY I TEORETICEHSKOY FIZIKI, Vol 25, 1977, p 41.
3. A. Yariv, J. OPT. SOC. AMER., Vol 66, 1976, p 301.

4. R. W. Hellwarth, J. OPT. SOC. AMER., Vol 67, 1977, p 1.

5. D. M. Bloom, P. F. Liao, N. P. Economou, OPTICS LETTS, Vol 1, 1977, p 58.

6. O. Yu. Nosach, V. I. Popovichev, V. V. Ragul'skiy, F. S. Fayzullov, PIS'MA V ZHURNAL EKSPERIMENTAL'NOY I TEORETICHESKOY FIZIKI, Vol 16, 1972, p 617.

7. V. Wang, G. R. Giuliano, OPTICS LETTS, Vol 2, 1978, p 4.

8. Yu. N. Kruzhilin, KVANTOVAYA ELEKTRONIKA, Vol 5, 1978, p 625.

9. H. Kogelnik, T. Li, APPL. OPTICS, 1966, p 1550.

10. G. A. Karillov, S. B. Kormer, G. G. Kochemasov, S. M. Kulikov, V. M. Murugov, V. D. Nikolayev, S. A. Sukharev, V. D. Urlin, KVANTOVAYA ELEKTRONIKA, Vol 4, 1975, p 666.

6610
CSO: 8144/1407 END